We are IntechOpen, the world's leading publisher of Open Access books Built by scientists, for scientists

4,800
Open access books available

122,000
International authors and editors

135M
Downloads

Our authors are among the

154
Countries delivered to

TOP 1%
most cited scientists

12.2%
Contributors from top 500 universities

CLARIVATE ANALYTICS BOOK CITATION INDEX INDEXED

WEB OF SCIENCE™

Selection of our books indexed in the Book Citation Index in Web of Science™ Core Collection (BKCI)

Interested in publishing with us?
Contact book.department@intechopen.com

Numbers displayed above are based on latest data collected.
For more information visit www.intechopen.com

4

Development of Granular Catalysts and Natural Gas Combustion Technology for Small Gas Turbine Power Plants

Zinfer R. Ismagilov[1], Mikhail A. Kerzhentsev[1], Svetlana A. Yashnik[1], Nadezhda V. Shikina[1], Andrei N. Zagoruiko[1], Valentin N. Parmon[1], Vladimir M. Zakharov[2], Boris I. Braynin[2] and Oleg N. Favorski[2]

[1]*Boreskov Institute of Catalysis, 630090, Novosibirsk*

[2]*Central Institute of Aviation Motors, Moscow*

Russia

1. Introduction

Gas turbine power plants (GTPPs) of low power (tens of kW to 1.5-2 MW) are promising autonomous sources of energy and heat. The application of gas turbine technologies saves fuel, solves heat supply and water shortage problems. The nominal efficiency of GTTPs belonging to different generations varies from 24% to 38% (average weighted efficiency – 29%). This is 1.5 times higher than that of combined heat power plants.

The main GTPP drawback is significant emission of toxic nitrogen oxides due to high temperature combustion of the gas fuel. The main approach used today to decrease the emission of nitrogen oxides from GTPPs is based on the use of the so-called homogeneous combustion chambers working with premixed lean fuel-air mixtures with two-fold excess of air. The decrease of NO_x formation is principally the result of the low flame temperatures that are encountered under lean conditions (Correa 1992). This technology makes it possible to decrease significantly the temperature in the combustion zone relative to traditional GTPP combustion chambers with separate supply of fuel and air to the combustion zone. As a result, the concentration of nitrogen oxides in the flue gases decreases from 100 ppm to 10-20 ppm. The downside of this approach is, however, that it results in low heat release rates, which, in turn, may negatively affect combustion stability.

The most efficient way to decrease emissions of nitrogen oxides in GTPPs is to use catalytic combustion of fuel (Trimm, 1983; Pfefferle & Pfeferle., 1987; Ismagilov & Kerzhentsev 1990; Parmon et al., 1992; Ismagilov et al., 1995; Ismagilov & Kerzhentsev, 1999; Ismagilov et al., 2010). In the catalytic chamber, efficient combustion of homogeneous fuel-air mixture is achieved at larger excess of air and much lower temperatures in the zone of chemical reactions compared to modern homogeneous combustion chambers.

In the last decade, the obvious advantages of the catalytic combustion chambers in GTPPs initiated intense scientific and applied studies in the USA (Catalytica) and Japan (Kawasaki Heavy Industries) which are aimed at development of such chambers for GTPPs for various applications (Dalla Betta et al., 1995; Dalla Betta & Tsurumi, 1995; Dalla Betta & Rostrup-Nielsen, 1999; Dalla Betta & Velasco, 2002).

The catalyst in a gas-turbine combustor has to withstand continuous operation for at least 10,000 h under severe operation conditions: high gas hourly space velocity (GHSV) and temperatures over 1200 K (McCarty et al., 1999). Material development is therefore one of the key issues in the development of catalytic combustion for gas turbines. Such catalyst has to possess high mechanical strength and the ability to initiate methane oxidation in lean mixtures at low temperatures 620-720 K and maintain stable oxidation during long time at temperatures above 1200 K (Dalla Betta et al., 1995; Dalla Betta & Rostrup-Nielsen, 1999).
Today catalysts for gas turbines are prepared in the form of monoliths from foil made of special corrosion-resistant alloys with deposited porous support and the active component based on platinum and/or palladium (Dalla Betta et al., 1995a; McCarty et al. 2000; Carroni et al. 2003). However, application of such catalysts requires many problems to be solved. The main problems are related to the high temperature of gas typical for modern gas turbines that requires the catalyst to operate at temperatures exceeding 1200 K for prolonged periods of time (total operation time of modern GTPPs reaches 100000 hours) (McCarty et al., 1999). The use of metal supports at temperatures above 900°C is limited due to possible thermal corrosion, especially in the presence of water vapor. It results in the catalyst destruction, peeling of the support and loss of noble metals decreasing the catalytic activity and shortening the catalyst lifetime. So, the improvement of the catalyst stability is an urgent problem.
One of the approaches to solve this problem is based on development of catalysts on granulated supports and design of a catalytic package for GTPP combustion chamber, which would provide minimum emissions of NO_x, CO and HC at moderate temperatures (930-950°C). In this chapter we present our results on development and study of alternative granular catalysts with reduced Pd content for methane catalytic combustion in mini gas turbines of 400-500 kW power with regenerative cycle, intended for decentralized power supply. The small power of these turbines results in reduced catalyst loading and makes possible the use of granular catalysts which are less expensive and can be easily manufactured using existing industrial facilities.

2. Selection of catalysts for application in gas turbine combustors

The most available fuel for GTPPs is natural gas, which consists largely of methane, which is the least readily oxidizable hydrocarbon. Therefore, it is necessary to produce catalysts capable of initiating methane oxidation at minimum possible temperatures and withstanding long-term exposure to temperatures above 930°C.
It is very difficult to find catalysts meeting requirements of both high activity at low temperature and good thermal stability at high temperatures. Therefore, in catalytic gas combustors generally staged combustion is employed: a highly reactive catalyst for the low-temperature (350 °C < T_{in} < 450 °C) conversion of CH_4 must be combined with a second catalyst which converts fuel at higher temperatures (T_{in} approx. 700 °C, T_{out} > 900 °C) (Carroni et al. 2002).
It is well known that catalysts based on noble metals are most active in oxidation reactions. They can initiate combustion at low temperatures, but it is inappropriate to use them above 750°C because of a high volatility of the noble metals (Arai et al. 1986). Use of palladium as the active component in the high-temperature oxidation of methane is most promising. This is because palladium has a high specific activity in this reaction (Burch & Hayes, 1995; Lee & Trimm, 1995) and a relatively low volatility in comparison with other noble metals, as was

determined by studying the interaction of the metals with oxygen at 730–1730°C (McCarty et al., 1999). It is these properties of palladium that attract researchers' interest to its behavior in the methane oxidation reaction. It is well known that, up to 800° C, palladium exists as PdO_x which undergoes reduction to palladium metal as the temperature is further raised. This reaction is reversible up to ca. 900°C, so a decrease in temperature leads to the reoxidation of Pd to PdO_x in air. As a consequence, the temperature dependence of the methane conversion always shows a hysteresis (Farrauto et al., 1992). There is still no consensus as to what form of oxidized palladium — bulk PdO, Pd with oxygen chemisorbed on its surface, or Pd particles covered by PdO —is the most active species in combustion ((McCarty, 1995; Burch, 1996; Su et al., 1998a; Su et al., 1998 b; Lyubovsky & Pfefferle, 1998; Lyubovsky & Pfefferle, 1999).

Supporting of palladium on a substrate, primarily γ- or α-Al_2O_3 or Al_2O_3 modified with rare-earth metal oxides, raises the activity and thermal stability of the catalyst through an increase in the degree of dispersion of the active component and in its aggregation stability (Baldwin & Burch, 1990; Groppi et al., 1999, Ismagilov et al., 2003, Ozawa et al., 2003, Liotta & Deganello, 2003; Yue et al., 2005).

Alternative catalytic systems for methane combustion are catalysts based on hexaaluminates and transition metal oxides. Hexaaluminates are the class of compounds with a general formula $AB_xAl_{12-x}O_{19}$, where A is a rare-earth or alkaline-earth metal, such as La and Ba, and B is a transition metal with an atomic radius comparable to the radius of aluminum (B = Mn, Co, Fe, Cr, Ni) (Machida et al., 1987; Machida et al., 1989). Hexaaluminates form from oxides at temperatures above 1200°C, and this is why they are very stable up to high temperatures. The specific surface area of hexaaluminates and, accordingly, their activity in methane oxidation depend on the preparation method (Chouldhary et al., 2002). However, irrespective of their specific surface area, the hexaaluminates are much less active than the palladium catalysts. In view of this, there have been attempts to enhance the catalytic activity of hexaaluminates by introducing Pd (Jang et al., 1999). In our earlier work (Yashnik et al. 2006), it was shown that introducing 0.5 wt % Pd into the hexaaluminate $(Mn,Mg)LaAl_{11}O_{19}$ resulted in a significant increase in the catalyst activity expressed as a 110°C decrease in the temperature of 50% methane conversion ($T_{50\%}$). In addition, a synergistic effect in the Pd–$(Mn,Mg)LaA_{11}O_{19}$ system was detected.

It was demonstrated earlier that thermally stable catalysts could be prepared from manganese oxides (Tsikoza et al., 2002; Tsikoza et al., 2003). The activity of these catalysts in hydrocarbon oxidation can be enhanced by their calcination at 900–1100°C. In our works (Tsikoza et al., 2002; Tsikoza et al., 2003), it was found that Mn–Al–O catalysts supported on γ-Al_2O_3 containing χ-Al_2O_3 and modified with Mg, La, or Ce were more active and thermally more stable (up to 1300°C) than the same catalysts supported on pure γ-Al_2O_3. We believe that the high degree of disorder of the χ-Al_2O_3 structure in comparison with γ-Al_2O_3 favors deeper interaction of manganese and modifiers with the support at the impregnation and low-temperature calcination stages. This yields Mn–Al–O compounds of complex composition (solid solutions and/or hexaaluminates) at 1300°C, due to which the catalysts are stable and highly active in methane oxidation.

Thus, based on literature data and our research results, two types of catalysts were selected for further development and study: (1) active Pd catalysts with low ignition temperature for initiation of methane combustion and (2) thermally stable hexaaluminate catalysts for methane combustion at temperatures over 900°C.

3. Synthesis of granular catalysts for methane combustion

3.1 Preparation of catalysts

In catalyst preparation, we used γ-alumina supports developed at the Boreskov Institute of Catalysis (Shepeleva et al., 1991; Ismagilov et al., 1991, Koryabkina et al., 1991; Koryabkina et al., 1996) prepared in the form of spheres and rings. Their characteristics are presented in Table 1.

Property	Spherical Al_2O_3	Ring-shaped Al_2O_3
Diameter, mm	2.2–2.5	7.5
Length, mm	-	7.5
Inner diameter, mm	-	2.5
Bulk density, g/cm^3	0.8	0.7
Pore volume (H_2O), cm^3/g	0.45	0.45
Specific surface area, m^2/g	180	200
Crushing strength under static conditions, kg/cm^2	270	23
Phase composition	γ-Al_2O_3	60% γ-Al_2O_3 40% χ-Al_2O_3

Table 1. Physicochemical properties of the spherical and ring-shaped aluminas

Pd–Ce–Al_2O_3. The catalyst was prepared on the ring-shaped support and contained 12 wt %CeO_2 and 2 wt % Pd. It was prepared by the incipient-wetness impregnation of the support with a cerium nitrate ($Ce(NO_3)_3 \cdot 6H_2O$) solution and then with an aqueous $Pd(NO_3)_2$ solution. Before being loaded with palladium, the alumina support modified with cerium was calcined at 600°C. After supporting of palladium, it was additionally calcined at 1000°C. The pilot catalyst batch was designated IK-12-60-2.

Mn–Al_2O_3.The catalyst was prepared on the ring-shaped support by the incipient wetness impregnation of the support with an aqueous manganese nitrate ($Mn(NO_3)_{2*} 6H_2O$) solution. It contained 11 wt % manganese oxides in terms of MnO_2. The catalyst calcination temperature was 900°C. It was similar in composition to the commercial catalyst IKT-12-40; for this reason, its pilot batch is hereafter designated IKT-12-40A.

Mn-La–Al_2O_3. This catalyst was prepared on the ring-shaped support by successive incipient-wetness impregnation of alumina with lanthanum and manganese nitrate solutions using the procedure described in (Yashnik et al., 2006). It contained 8–11 wt % manganese in terms of MnO_2 and 10–12 wt % lanthanum in terms of La_2O_3. These concentrations of manganese and lanthanum are sufficient to ensure a high catalytic activity and stability of the catalyst (Yashnik et al., 2006). The calcination temperature was 1000°C, lower than the temperature used in our previous study (Yashnik et al., 2006) and was equal to the onset temperature of hexaaluminate phase formation. This allowed us to increase the specific surface area of the sample. The pilot catalyst batch was designated IK-12-61.

Pd–Mn–La–Al_2O_3. This catalyst was prepared on the ring-shaped support by successive incipient-wetness impregnation with lanthanum and manganese nitrate solutions. Next, the samples were dried and calcined at 400°C. Thereafter, the samples were loaded with a palladium nitrate solution by impregnation. Final calcination was carried out at 1000°C. The resulting catalyst contained 8–11 wt % Mn in terms of MnO_2, 10–12 wt % La in terms of La_2O_3, and was 0.65 wt % Pd. The pilot batch of the catalyst was designated IK-12-62-2.

3.2 Characterization of catalysts

When developing and optimizing the catalysts based on manganese oxides, including those additionally containing lanthanum and palladium, we investigated how their physicochemical and catalytic properties depend on their chemical composition, the active component and modifier (manganese, lanthanum, palladium, and hexaaluminate phase) contents, the chemical nature of Mn and Pd precursors, the calcination temperature, and the active component introduction method (Yashnik et al., 2006; Tsikoza et al., 2002; Tsikoza et al., 2003). Measuring the catalytic activity of catalyst samples in methane oxidation allowed us to find the optimal catalytic systems, whose properties are listed in Table 2.

The catalysts on the ring-shaped alumina support (IK-12-60-2, IKT-12-40A, IK-12-61, IK-12-62-2) were tested in natural gas combustion at 930°C in the pilot plant at the Boreskov Institute of Catalysis.

The results of these tests are presented in Table 3. The catalyst IK-12-60-2 retained its high activity over 100 h: the ignition temperature (T_{ign}) was 240°C, and the reaction products were almost free of CO and NO_x. The manganese-containing catalysts were less active: with these catalysts, T_{ign} and the residual CO and NO_x contents were higher than with IK-12-60-2. However, the initial activity of the catalyst IK-12-61 did not decrease, but even gradually increased during testing: in 200 h, T_{ign} falls from 365 to 350°C, the NO_x concentration in the reaction products remained at the 0–1 ppm level, and the CO concentration decreased from 55 to 34 ppm. The catalyst IK-12-61 modified with 0.65 wt % palladium (IK- 12-62-2) allowed us to reduce the ignition temperature of the methane–air mixture almost by 100°C and the CO concentration in the reaction products by more than one order of magnitude. Service life tests suggested that all catalysts are tolerant to high temperatures (up to 930°C) and to the action of the reaction medium. The ignition temperature and the methane–air combustion efficiency remained unchanged at least over 100 h of testing.

The investigation of the physicochemical properties of the initial samples (Table 2) showed that, in IK-12-60-2, the active component PdO is finely dispersed and this allows one to initiate combustion of the methane–air mixture at low temperatures.

The initial catalysts based on Mn and La oxides (IK-12-61 and IK-12-62-2) contain the hexaaluminate phase, which is known to be resistant to high temperatures. The durability tests altered the structural and textural characteristics of the catalysts (Table 4). Over the first 50 h of testing, the specific surface area and pore volume of the IK-12-60-2 catalyst decreased because of the coarsening of alumina particles and the onset of α-Al_2O_3 formation via the δ-Al_2O_3 – α-Al_2O_3 phase transition under prolonged heating. The active component PdO underwent partial decomposition to Pd^0. In the next 50 h, the textural parameters stabilized and the degree of dispersion of the remaining PdO phase increased. The degree of dispersion of metallic Pd^0 decreased with testing time. The Mn catalysts are more tolerant to high temperatures and are less prone to aggregation than the Pd–Ce catalyst. Some changes in the phase composition of the catalysts occur because of the formation of high-temperature phases, namely, α-Al_2O_3 and a (Mn, Al)Al_2O_4 solid solution in IKT-12-40A and manganese hexaaluminate in IK-12-61 and IK-12-62-2.

The catalytic activity of the hexaaluminate-based samples in the CH_4 oxidation reaction after 100-h-long testing was similar to the activity of the fresh catalysts: T_{50} is 470–480°C for the catalyst IK-12-61 and 363–380°C for IK-12-62-2 at GHSV = 1000 h^{-1} (Fig. 1). The activity of the catalysts Pd–Ce–Al_2O_3 and MnO_x–Al_2O_3 decreased slightly, and T_{50} increased by 50°C.

Catalyst	Calcination temperature, °C	Chemical composition, wt %	Phase composition*	S_{sp},** m^2/g	V_Σ (N_{ads})***, cm^3/g	Strength, kg/cm^2	T, $_{50\%\ CH4}$,**** °C
IK-12-60-2	1000	Pd – 2.1 Ce – 10.1	δ-Al_2O_3, CeO_2 (~200 Å, S_{33}=1100), PdO (~180 and 250 Å, S_{39} = 480)	74	0.26	24	330
IKT-12-40A	900	Mn – 6.9	Mixture of (δ + γ)-Al_2O_3, α-Al_2O_3, Mn_2O_3	80	0.23	23	400
IK-12-61	1000	Mn – 6.9 La – 10.1	$MnLaAl_{11}O_{19}$ (S_{37} = 60), $LaAlO_3$, γ-Al_2O_3#	43	0.18	34	420
IK-12-62-2	1000	Pd – 0.65 Mn – 7.1 La – 9.4	$MnLaAl_{11}O_{19}$ (S_{37} – traces),γ-Al_2O_3 (a = 7.937 A),PdO (~400 A, S_{39} = 70)	48	-	25	385

*The particle size was derived from the size of coherent-scattering domain region. Relative phase contents were estimated from peak areas (S_i, arb.units) in diffraction patterns. γ-Al_2O_3# is a solid solution based on γ-Al_2O_3. ** S_{sp} is specific surface area, ***V_Σ (N_{ads}) is pore volume found form N_2 adsorption, ****T, $_{50\%\ CH4}$ is temperature of 50% methane conversion on catalyst fraction 0.5-1.0 mm at GHSV = 1000 h^{-1} and methane concentration in air equal to 1%.

Table 2. Physicochemical and catalytic properties of the initial catalysts on spherical and ring-shaped supports

Catalyst	Test duration, h	T_{ign}, °C	Residual content, ppm	
			CO	NO_x
IK-12-60-2	100	240	0-1	0-1
IKT-12-40A	100	350	84-55	0-1
IK-12-61	200	365-350	55-34	0-1
IK-12-62-2	200	290	2-3	0-1

Table 3. Results of catalyst durability tests in natural gas combustion at 930°C in a bench testing unit at the Boreskov Institute of Catalysis

The catalytic activity of the hexaaluminate-based samples in the CH_4 oxidation reaction after 100-h-long testing was similar to the activity of the fresh catalysts: T_{50} is 470–480°C for the catalyst IK-12-61 and 363–380°C for IK-12-62-2 at GHSV = 1000 h^{-1} (Fig. 1). The activity of the catalysts Pd–Ce–Al_2O_3 and MnO_x–Al_2O_3 decreased slightly, and T_{50} increased by 50°C.

Catalyst	Test duration, h	Phase composition	S_{sp}, m^2/g	V_Σ (N_{ads}), cm^3/g	Strength, kg/cm^2
IK-12-60-2	50	δ-Al_2O_3, α-Al_2O_3 (traces), CeO_2 (~200 Å, S_{33} = 1100), PdO (~ 300 Å, S_{39} = 180), Pd^o (~ 300 Å, S_{47} = 120)	42	0.18	21
	100	δ-Al_2O_3, α-Al_2O_3 (traces), CeO_2 (~200 Å, S_{33} = 1100), PdO (~ 160 Å, S_{39} = 180), Pd^o (~500 Å, S_{47} = 80)	38	0.17	19
IKT-12-40A	100	α-Al_2O_3, γ-Al_2O_3-based solid solution (Mn, Al)Al_2O_4 (a = 8.151 Å)	66	0.22	19
IK-12-61	30	$MnLaAl_{11}O_{19}$ (S_{37} = 240), $LaAlO_3$, α-Al_2O_3	41	0.18	30
	50	$MnLaAl_{11}O_{19}$ (S_{37} = 250), $LaAlO_3$, α-Al_2O_3	33	0.15	28
	100	$MnLaAl_{11}O_{19}$ (S_{37} = 240), $LaAlO_3$, α-Al_2O_3	31	0.13	28
IK-12-62-2	50	$MnLaAl_{11}O_{19}$ (S_{37} = 230), γ-Al_2O_3# (a = 7.937 Å), Pd^o (S_{41} = 90), PdO (400 Å, S_{39} = 160)	31	-	29
	100	$MnLaAl_{11}O_{19}$ (S_{37} = 230), γ-Al_2O_3# (a = 7.937 Å), Pd^o (>400 Å, S_{47} = 40), PdO (>400 Å, S_{39} = 160)	30	-	32
	200	$MnLaAl_{11}O_{19}$ (S_{37} = 340), γ-Al_2O_3# (a = 7.937 Å), α-Al_2O_3 (S_{29} = 30), PdO (>400 Å, S_{39} = 180), Pd^o (>400 Å, S_{47} = 40)	30	-	35

Table 4. Physicochemical properties of the catalysts after durability tests in natural gas combustion

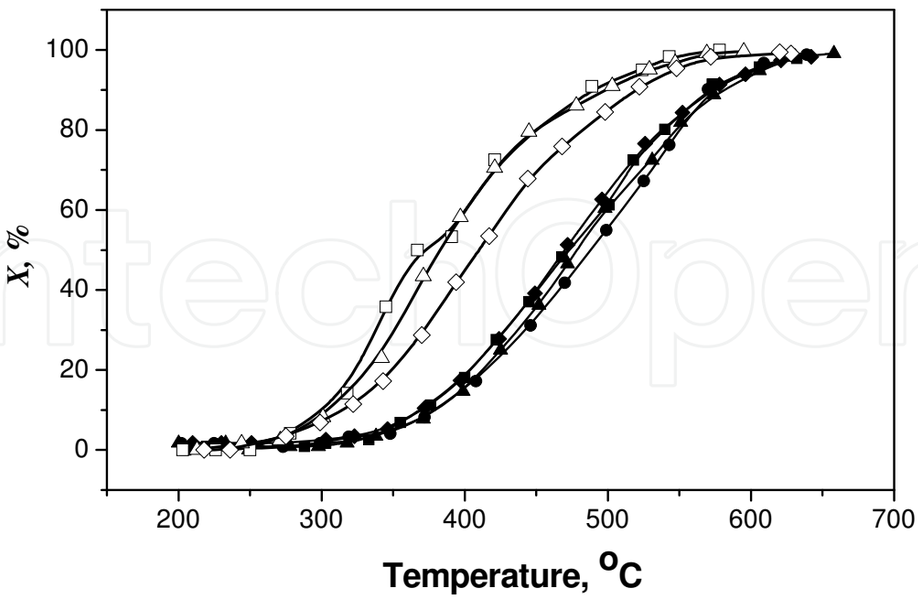

Fig. 1. Temperature dependences of methane conversion (1 vol % CH_4 in air, GHSV=1000 h^{-1}) on the catalysts: IK-12-61: ▲ – initial; ●-after 30 h; ■ - after 50 h; ◆ - after 100 h testing in CH_4 combustion at 930°C; IK-12-62-2: △- initial; □- after 50 h; ◊- after 100 h testing.

4. Kinetic studies of methane catalytic oxidation

Kinetic studies of methane catalytic oxidation were performed in a flow reactor. The reaction order with respect to methane was found to be equal to 1. In kinetic calculations, we used activity data for the 0.5–1.0 mm size fractions of the catalysts in methane oxidation at GHSV = 1000, 24000, and 48000 h^{-1}. The results obtained by data processing in the plug flow approximation are presented in Table 5. The obtained kinetic parameters were used further for modeling of methane combustion.

Catalyst	k_0, s^{-1}	E, kJ/mol
IK-12-60-2	4.36×10^7	81.4
IKT-12-40A	1.09×10^5	71.2
IK-12-61	1.09×10^5	71.2
IK-12-62-2	3.29×10^5	63.8

Table 5. Kinetic parameters of the total methane oxidation reaction

5. Experimental studies of natural gas combustion in a catalytic combustion chamber

5.1 Experimental procedures

Experimental studies of natural gas combustion were carried out in a stainless-steel tubular vertical catalytic combustion chamber (CCC) with an internal diameter of 80 mm. The CCC is schematically shown in Fig. 2. The volume of the catalytic package was 1.3 L.

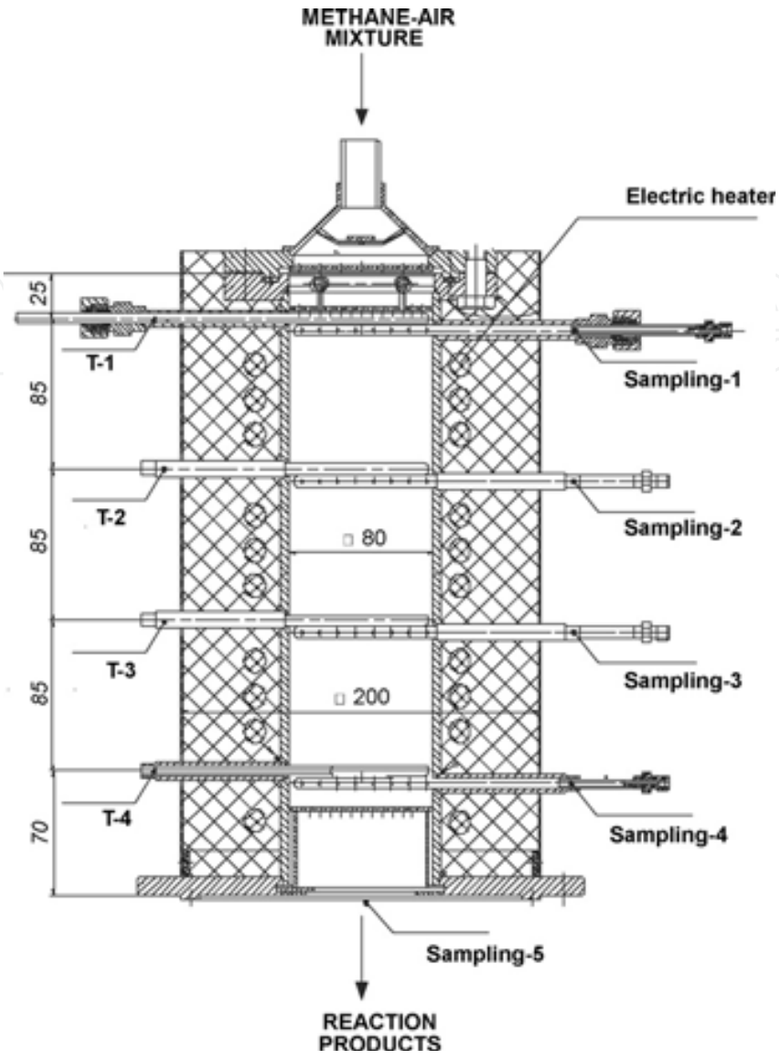

Fig. 2. Schematic view of the catalytic combustion chamber: T-1 to T-4: thermocouples, sampling 1–5: gas samplers.

The air/fuel equivalence ratio (α) was selected to be close to the minimum value of this parameter in the operating regime of full-power GTPP (α= 6.4–6.8). The inlet temperature of the fuel–air mixture (T_{in}) was varied between 470 and 600°C, the temperature at the chamber exit (T_{ex}) was 900–985°C, the GHSV of the fuel–air mixture was 8500–15,000 h^{-1}.

Natural gas was introduced into the combustion chamber after reaching the light-off temperature. Due to the natural gas combustion, the temperature in the catalyst bed increased and reached the values close to the desired ones in 30–40 min. The temperature mode was corrected by smooth variation of the air and natural gas flows.

When the desired temperature regime was reached, temperatures along the length of the catalytic chamber were measured. The radial temperature profile was measured before and after the pilot-plant tests. A reference manometer was used to measure the pressures in the catalyst bed. The gas phase composition at the CCC outlet was analyzed using a "Kristall-2000 M" gas chromatograph. The gas probes were also analyzed in parallel using ECOM-AC gas analyzer.

The catalytic packages studied are schematically presented in Fig. 3.

1. uniform loading with ring shaped high temperature resistant oxide catalyst
2. two high temperature catalysts with different granule shape. According to the results of modeling, the methane conversion should increase with change of granule shape as: ring < cylinder < sphere. However, the use of spherical catalyst for entire reactor is impossible due to a high pressure drop. Therefore, the reactor consists of two sections: the first with ring shaped oxide catalyst (or Pd-Mn-Al-O) and the second downstream section with spherical catalyst having lower fractional void volume. This combination with a short bed of spherical catalyst provides rather high methane combustion efficiency at a minor increase of pressure drop.
3. two ring shaped catalysts with different catalytic activity. In this case, a short bed (ca.10%) of the highly active Pd-Ce-catalyst is located in the upstream section at low temperature, and it initiates methane combustion. The larger bed of high temperature resistant oxide catalyst in the downstream section provides high efficiency of methane combustion. This design of catalytic reactor allows a reduction of total Pd loading and an increase of methane combustion efficiency at a low inlet temperature.
4. three catalysts with different catalytic activity and fractional void volume. The highly active Pd-catalyst in the upstream section initiates methane oxidation, the high temperature resistant catalyst in the larger middle section provides stable methane combustion. The bicomponent spherical Pd-Mn-Al-O catalyst with a low Pd-content and low fractional void volume in the downstream section improves the efficiency regarding the residual traces.

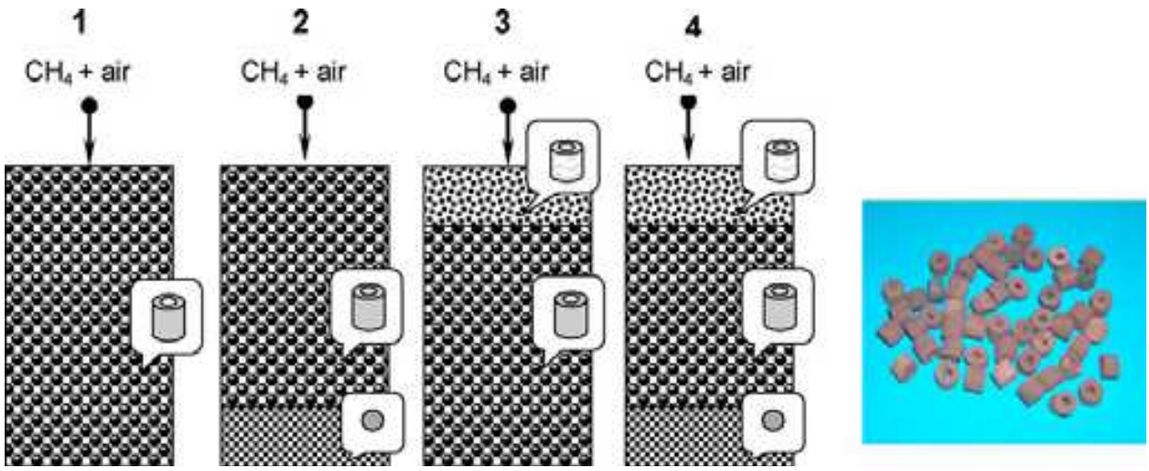

Fig. 3. Schemes of uniform (1) and structured (2–4) loading of the reactor and photo of granulated catalyst (Yashnik et al., 2009, Ismagilov et al., 2010)

5.2 Tests of the catalytic combustion chamber with uniform catalyst package

First, we tested CCC loaded with one catalyst. Such loading will be hereafter denoted as "uniform" and provides for one-stage combustion of the natural gas–air mixture. Such experiments allowed us to analyze the perspectives of using manganese–alumina catalysts and evaluate their catalytic properties in natural gas combustion by such parameters as outlet temperature and emission of hydrocarbons. Mn–Al_2O_3, Mn–La–Al_2O_3 and Pd–Mn–La–Al_2O_3 catalysts shaped as rings were tested for 72–120 h in a temperature cycle mode.

The temperature cycle mode consisted of four cycles of gas combustion, catalyst cooling and repeated start of the combustion process. The combustion process was carried out at GHSV= 15,000 h^{-1} and inlet temperature 580–600 ◦C. The value of α was maintained at 6.8–6.9. The height of the catalytic package was 300 mm. The dynamics of changes in the activity of different catalysts are presented in Fig. 4.

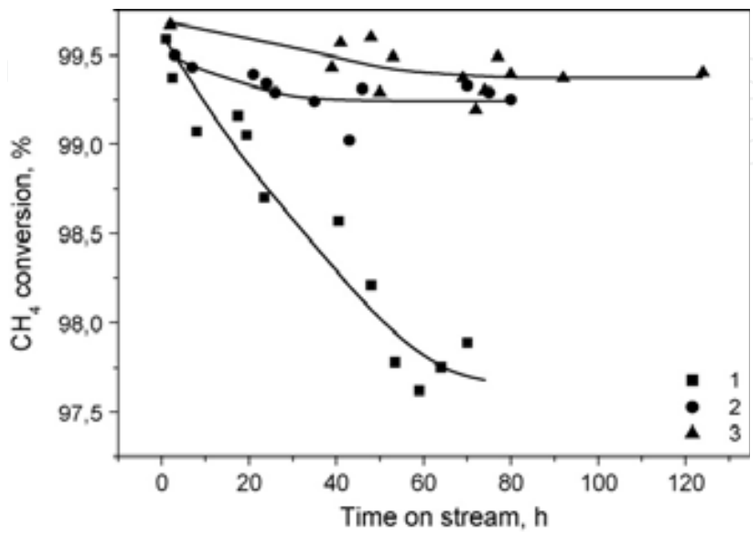

Fig. 4. Methane conversion vs. operation time in CCC at GHSV: 14,900–15,100 h^{-1} and α = 6.7–6.8. Uniform catalyst package loaded with: (1) Mn–Al_2O_3 (T_{in} – 600 °C); (2) Mn–La–Al_2O_3 (T_{in} – 600 °C); (3) Pd–Mn–La–Al_2O_3 (T_{in} – 575–580 °C).

The data presented in Fig. 4 indicate that the catalysts Mn–Al_2O_3, Mn–La–Al_2O_3 and Pd–Mn–La–Al_2O_3 differ both by their activity and stability. For example, the activity of the Mn–Al_2O_3 catalyst gradually decreased as evidenced by gradual increase of the methane and CO concentration at the CCC outlet. The methane conversion decreased from 99.6% to 97.9% during the first 50–54 h on stream. Then the catalyst activity stabilized and did not change in the following 80 h on stream (Fig. 4, curve 1). At the end of the experiment the methane and CO concentrations stabilized at 330 and 110 ppm, respectively (Table 6).

Table 6 compares the outlet temperatures and emissions of CH_4 and CO during natural gas combustion over Mn–Al_2O_3 catalysts with different fractional compositions at GHSV= 8500–15,000 h^{-1}.It was shown that the methane combustion efficiency over large catalyst granules with the external ring diameter 15mm was low.

Even at a low load on the catalyst (GHSV = 8500 h^{-1}) the methane conversion was 97% whereas the methane and CO emissions at the outlet were 500 and 300 ppm, respectively. Note that under similar CCC operation conditions the application of catalyst granules with the external diameter 7.5 mm allowed for a 10-fold decrease of the methane emission and 30-fold decrease of the CO emission. In both cases the CCC efficiency also depended on contact time. The contact time increase from 0.24 s (GHSV = 15,000 h^{-1}) to 0.42 s (GHSV = 8500 h^{-1}) affected more significantly the efficiency of CCC loaded with the catalyst with smaller internal and external diameters of the granules (7.5 mm), i.e. lower fractional void volume of the catalyst bed. These data indicate that the mass transfer of the reagents and reaction products to/from the catalyst surface substantially affects the total CCC efficiency in methane combustion at the inlet temperature 600 ◦C. At this temperature methane

oxidation proceeds mainly on the catalyst surface and the contribution of homogeneous reactions is negligible, which is confirmed by substantial improvement of methane conversion with the increase of the catalysts geometrical surface.
These data agree with the work (Hayashi et al., 1995) where the authors showed the dependences of relative contributions of heterogeneous and homogeneous methane oxidation reactions on the monolithic Pt–Pd catalyst on the inlet temperature, pressure and the catalyst channel density. Placing the catalysts with small cells (200 cpsi) in the front part of the reactor allowed the increase of heat release there at 600 °C (Hayashi et al., 1995), at the same time in the monolith with larger channels (100 cpsi), especially at temperature 700 °C the homogeneous oxidation reaction was prevailing.

Fraction, mm	G_{air}, m^3/h	G_{NG}, l/h	GHSV, h^{-1}	α	T_{in} °C	T_1* °C	T_2* °C	T_3* °C	T_4* °C	C_{CH4}, ppm	C_{CO}, ppm	C_{NOx} ppm	X_{CH4} %
7.5	19.4	309	14900	6.78	577	659	867	920	917	328	102	1	97.89
7.5	15.0	243	11500	6.70	567	677	903	926	905	164	41	2	98.68
7.5	11.1	180	8500	6.67	571	728	923	925	896	48	9	1	99.69
15	19.2	324	14800	6.41	590	623	763	898	918	987	943	1	93.87
15	15.0	267	11500	6.10	570	604	783	909	919	630	616	2	96.28
15	11.1	204	8500	5.90	562	591	790	903	897	504	344	2	97.13

G_{air} is volume flow rate of air, G_{GN} is volume flow rate of natural gas, C_{CH4}, C_{CO}, C_{NOx} are outlet concentrations of CH_4, CO and NO_x; X_{CH4} is methane conversion, *temperatures measured by thermocouples placed along the catalyst bed at different distances from the CCC inlet: T_1 – 25 mm; T_2 – 110 mm; T_3 – 195 mm; T_4 – 280 mm.

Table 6. Parameters of methane combustion over Mn-Al_2O_3 catalysts with different fractional composition

The activity of Mn–La–Al_2O_3 and Pd–Mn–La–Al_2O_3 catalysts also decreased in the first 30–40 h on stream. However, the activity decrease was less dramatic compared to the Mn–Al_2O_3 catalyst (Fig. 4). The methane conversion over Mn–La–Al_2O_3 and Pd–Mn–La–Al_2O_3 catalysts decreased from 99.5% to 99.3% (Fig. 4, curve 2) and from 99.7% to 99.4% (Fig. 4, curve 3), respectively. The concentrations of methane and CO stabilized at 100 and 85 ppm, correspondingly. Note that the Pd–Mn–La–Al_2O_3 catalyst showed these values of the residual CH_4 and CO concentrations at a lower inlet temperature 575 °C than the Mn–La–Al_2O_3 catalyst that showed similar values at 600 °C inlet temperature. The NO_x concentration at the outlet of the catalyst package did not exceed 0–2 ppm on all the catalysts. Thus, the obtained results demonstrate that the activity of the Pd–Mn–La–Al_2O_3 catalyst was higher than that of the catalysts without Pd. Meanwhile, the stability of this catalyst was comparable to that of Mn–La–Al_2O_3 being determined by the Mn-hexaaluminate phase. The stability of these catalysts was much higher than that of the catalyst based on Mn oxide. These results of the catalysts testing under the above conditions are in good agreement with our results on the study of the catalysts activity in methane oxidation in a laboratory reactor (Yashnik et al., 2006; Tsikoza et al., 2002; Tsikoza et al., 2003). It was shown that modification of Mn-alumina catalysts with oxides of rare earth metals allowed a considerable increase of thermal stability of the catalysts due to the

formation of manganese–hexaaluminate phase (Yashnik et al., 2006; Tsikoza et al., 2002). Introduction of 0.5 wt.% Pd into Mn–La–Al_2O_3 resulted in a substantial decrease of the light-off temperature of the air–natural gas mixture (Yashnik et al., 2006).

The pressure drop on the full height of the catalyst bed for uniform loading of the catalysts in the form of 7.5 mm × 7.5 mm × 2.5 mm rings for the catalysts Mn–Al_2O_3, Mn–La–Al_2O_3 and Pd–Mn–La–Al_2O_3 was 35, 23 and 14 mbar at GHSV= 14,900, 11,500 and 8500 h^{-1}, respectively. These values are less 4% of the total pressure which was 1 bar.

Figure 5 shows the effect of the air/fuel equivalence ratio on the outlet temperature and methane conversion over the catalyst package loaded with the Mn–La–Al_2O_3 catalyst. The variation of α between 6.2 and 7.2 showed that its decrease (enrichment of the fuel–air mixture with methane) resulted in a growth of the temperature at the outlet of the catalyst bed and, consequently, increase of the methane conversion. For instance, when α was decreased from 7 to 6.2, the methane conversion increased from 99.3% to 99.93% and the temperature grew from 937 to 992 ◦C at GHSV= 15,000 h^{-1}. However, Fig. 5 shows that methane conversion above 99.9% was observed when the temperature in the catalyst bed exceeded 980°C. So high temperature is undesirable because the catalyst overheating during prolonged operation will inevitably lead to its deactivation. Therefore, alternative methods of increasing the methane conversion are required.

As it is known from the literature, one of the ways to increase the CCC efficiency is to use multistage (multizone) combustion. This method allows one to control the temperature profile by varying the catalyst activity in different zones of the catalytic combustion chamber. Several methods for stepwise combustion of hydrocarbon fuels in the GTPP CCC have been implemented. American companies Catalytica (Dalla Betta & Tsurumi, 1993) and Westinghouse Electric Corp. (Young & Carl, 1989) suggested feeding the fuel–air mixture to a monolith catalyst consisting of alternating channels with an active component and without it. If the surface reaction in the channel with a catalyst takes place in the diffusion-controlled regime, adiabatic heating to the flame temperature does not occur because the heat is transferred to the inert channel of the monolith. The fuel–air mixture exiting the inert channels is burnt at the exit of the monolith catalyst.

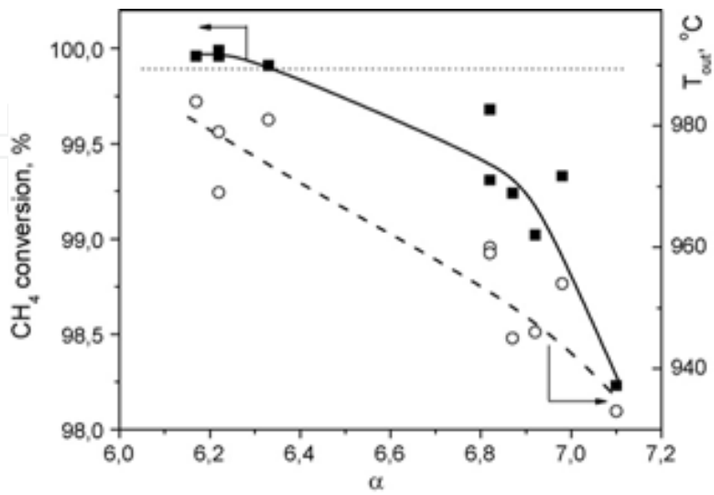

Fig. 5. Dependence of methane conversion (filled symbols) and catalyst temperature at the CCC outlet (open symbols) during methane combustion in CCC loaded with Mn–La–Al_2O_3 catalyst on α. GHSV= 15,000 h^{-1}, T_{in} = 600 °C.

In patents (Dalla Betta & Tsurumi, 1993; Pfefferle, 1997) it was suggested to use multi-section catalysts with different levels of activity to carry out combustion in the kinetically controlled regime. The catalytic activity is regulated by varying the concentration of the noble metal (most often Pd) in the range of 5–20 wt.% or the nature of the active component (noble metal, transition metal oxides). It was also suggested (Dalla Betta & Velasco, 2002) to use a two-stage monolithic catalyst combined from catalytic systems with different thermal stabilities. A catalyst with low ignition temperature requiring minimal heating is placed at the entrance zone whereas a catalyst resistant to the action of high temperatures is placed at the exit.

5.3 Tests of CCC with combined two-stage catalyst package

We suggested a design of a two-stage catalyst package consisting of catalysts with the same chemical composition but different fractional compositions. Using the Pd–Mn–La–Al_2O_3 catalyst as an example we studied the effect of the catalyst bed fractional void volume on the methane conversion in CCC. The main part of the catalyst package was loaded with the catalyst formed as 7.5 mm × 7.5 mm × 2.5 mm rings having the fractional void volume (ε) 0.52. A catalyst layer with 60 mm height consisting of 4–5 mm spherical granules with fractional void volume 0.42 was placed near the outlet of the package. The total Pd concentration in the catalyst package was 0.6 wt.%.

The application of the spherical catalyst at the CCC outlet made it possible to achieve over 99.9% combustion efficiency (Fig. 6) and decrease the methane concentration from 85 ppm to 0–5mm and the CO concentration to 4–8 ppm at inlet temperature 580°C and α in the range of 6.7–7.1. Fig. 7 presents the methane and CO profiles along the reactor length. One can see that more than 90% of methane is oxidized at the distance ca. 200 mm from the inlet. The maximum CO concentration is observed in this region. Further combustion of methane and CO to concentrations below 10 ppm is observed mostly at 280–340 mm from the inlet of

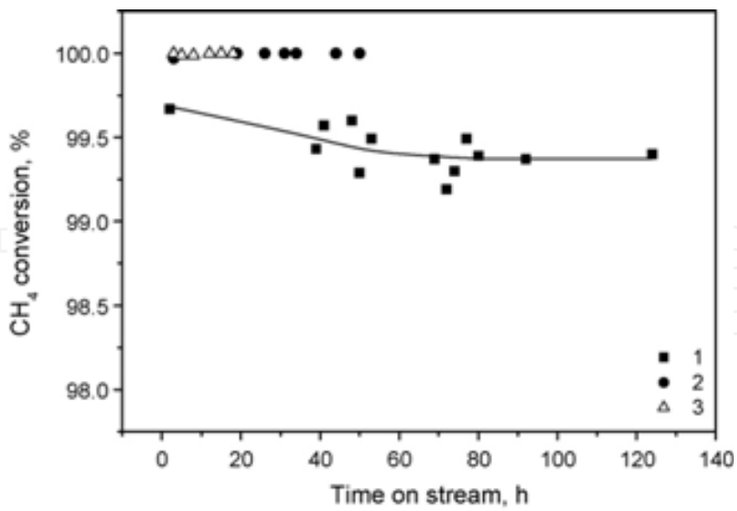

Fig. 6. Methane conversion vs. operation time in CCC for different catalyst packages: (1) uniform catalyst package Pd–Mn–La–Al_2O_3, rings (T_{in} = 575–580 ◦C, GHSV= 15, 100 h^{-1}, α= 6.8–6.9); (2) combined catalyst package: Pd–Mn–La–Al_2O_3, rings and spheres (Tin = 575–580 ◦C, GHSV= 12,500 h^{-1}, α = 6.7–6.8); (3) combined catalyst package: Mn–La–Al_2O_3, rings, and Pd–Mn–La–Al_2O_3, spheres (T_{in} – 575–580◦C, GHSV= 12,500 h^{-1}, α = 6.7–6.8).

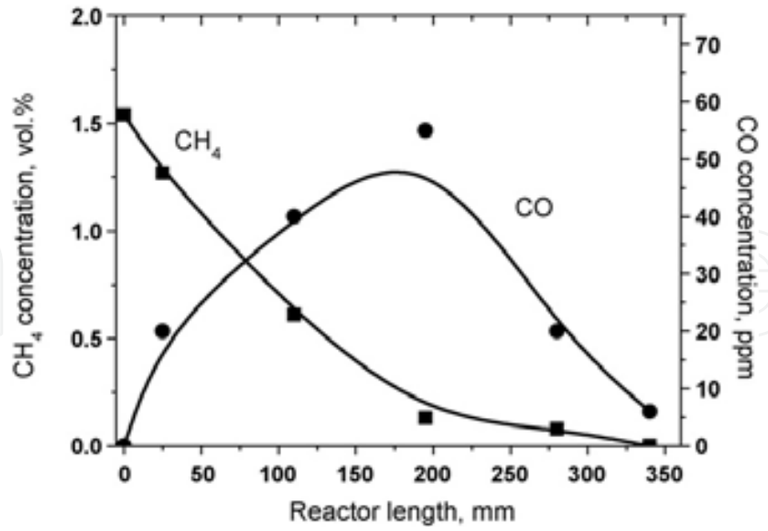

Fig. 7. Profiles of methane and CO concentrations along the reactor length during combustion of natural gas on a combined catalyst package Pd–Mn–La–Al_2O_3: 280 mm of rings and 60 mm of spherical granules (T_{in} = 580 ◦C, GHSV= 12,500 h^{-1}).

the catalyst package, i.e. in the area where the spherical catalyst is loaded. The layer of this catalyst has a higher density and higher geometrical area, which provides more efficient use of the catalyst, and thus increases the CCC efficiency.

Then, we determined the role of catalyst activity in the total CCC efficiency. We carried out tests on a combined catalyst package consisting on Mn–La–Al_2O_3 (rings) and Pd–Mn–La–Al_2O_3 (spheres) and compared the methane conversion with the results of the previous test. The ratio of the layer heights was similar to that used in the previous test – 280/60mm. The total Pd content in CCC was much lower - about 0.1 wt.% because most of the catalyst package consisted of the Mn–La–Al_2O_3 catalyst. The activity of this catalyst ($T_{50\%\ CH4}$) is lower than that of Pd–Mn–La–Al_2O_3 (Table 3). However, the substitution of the more active catalyst with a less active and a 6-fold decrease of the total Pd content (Fig. 6, curve 3) did not decrease the methane combustion efficiency compared to the previous test (Fig. 6, curve 2) where the total Pd content was 0.6 wt.%. Thus, increase of the efficiency of the use of the catalyst granules even at a relatively short length of the CCC results in a noticeable improvement of the overall CCC efficiency at a low total Pd loading.

However, such CCC design produced a larger pressure drop than the uniform catalyst package with ring-shaped catalysts. The pressure drop in the two-stage catalyst package was 48 mbar at GHSV= 12,500 h^{-1} and 30 mbar at GHSV= 10,000 h^{-1}. The pressure drop in the layer of the spherical Pd–Mn–La–Al_2O_3 catalyst was 20 and 13 mbar, respectively.

The tests of CCC with a combined two-stage catalyst package at lower inlet temperature showed that the inlet temperature decrease from 580 to 470 ◦C decreased the methane combustion efficiency. The methane conversion over the catalyst package Pd–Mn–La–Al_2O_3 (rings)/Pd–Mn–La–Al_2O_3 (spheres) decreased from 99.93% to 99.7% with methane and CO concentrations increasing to 37 and 150 ppm, respectively. The methane conversion over the catalyst package Mn–La–Al_2O_3 (rings)/Pd–Mn–La–Al_2O_3 (spheres) at the inlet temperature

470 ◦C was only 99.4% with methane and CO concentrations 90 and 220 ppm, respectively. The increase of the methane combustion efficiency at low inlet temperature was made possible by organizing a three-stage catalyst package.

5.4 Tests of CCC with combined three-stage catalyst package

In the three-stage catalyst package we placed a highly active Pd–Ce–Al_2O_3 catalyst with 2 wt.% Pd at the entrance zone. Most of the package consisted of Mn–La–Al_2O_3 catalyst. Both catalysts were shaped as 7.5 mm × 7.5 mm × 2.5 mm rings. Pd–Mn–La–Al_2O_3 catalyst in the form of 4–5 mm spherical granules was placed in the downstream part of the catalyst package. The ratio of the catalyst layer heights was 40/240/60mm. Similarly to the tests of two-stage packages, the ratio of the heights of ring and spherical granules was 280/60mm. The tests were carried out at the inlet temperature 470 ◦C, GHSV= 10,000 h^{-1} and α = 5.2. Under such conditions the temperature at the outlet zone of the catalyst package remained at about 950 ◦C.

Figure 8a shows the temperature profile along the CCC length. In the inlet zone filled with the Pd–Ce–Al_2O_3 catalyst at 25 mm from the inlet the feed is heated from 470 to 580 ◦C due to catalytic combustion of methane. The latter temperature is sufficiently high for effective functioning of the main Mn–La–Al_2O_3 catalyst bed. Further temperature growth from 580 to 950◦C takes place on this catalyst.

The profiles of the methane and CO concentrations along the CCC length are shown in Fig. 8b. The methane concentration profile shows a sharp concentration fall in the inlet zone where the Pd–Ce–Al_2O_3 catalyst is located. The main decrease of the concentration from 1.4% to 170 ppm takes place in the zone of the main catalyst Mn–La–Al_2O_3 (40–280 mm). Then at the CCC exit in the layer of the spherical Pd–Mn–La–Al_2O_3 catalyst the residual amounts of methane burn from 170 to 0–10 ppm concentrations. The concentration of the CO intermediate initially grows. Then, when most methane is oxidized, the CO concentration also decreases from 300 to 40 ppm in the Mn–La–Al_2O_3 bed. Finally, residual CO is burned in the spherical Pd–Mn–La–Al_2O_3 catalyst to 10 ppm concentrations. The pressure drop in the catalyst package was 29–30 mbar.

Thus, the use of the three-stage combined catalyst package including a thin layer of the active palladium–ceria catalyst located at the CCC entrance before the main oxide catalyst bed allows us to increase the CCC efficiency for methane combustion and obtain required low methane emission value of 10 ppm at low inlet temperature 470◦C. This additional catalyst layer provides the initial methane conversion and temperature increase before the main catalyst bed.

6. Modeling of methane combustion processes in a catalytic combustor

6.1 Model description

The catalytic packages used in modeling are schematically presented in Fig. 3. For calculation of the catalyst package performance, we used a model of a steady-state adiabatic plug-flow reactor. The calculation of the temperature profiles and methane conversion was performed at variation of catalyst methane oxidation activity and geometry of catalyst granules, ratio of bed lengths of different catalysts in the package, temperature, pressure and gas space velocity in the combustor.

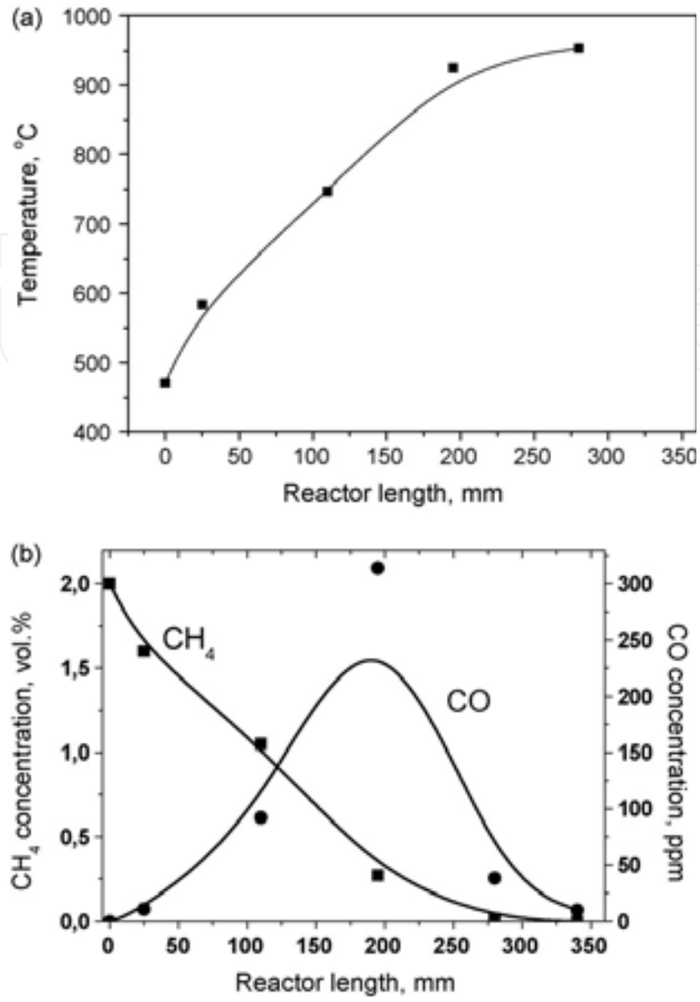

Fig. 8. Profiles of temperature (a) and methane and CO concentrations (b) along the reactor length during combustion of natural gas on a combined catalyst package Pd–Mn–La–Al_2O_3/Mn–La–Al_2O_3/Pd–Ce–Al_2O_3 (T_{in} = 470 ◦C, GHSV= 10,000 h^{-1}, α = 5.2).

The reaction rate was calculated using Eqs. (1) and (2):

$$W = k\, C_{CH_4} \left(\frac{P}{P_0} \right) \tag{1}$$

$$k = \eta\, k_0 (1-\varepsilon) \exp\left(-\frac{E/R}{T} \right) \tag{2}$$

where k is the kinetic constant (s^{-1}), C_{CH4} is the methane concentration (molar fraction), P is the operating pressure (bar), P_0 is the pressure (bar) at which the reaction kinetics is studied experimentally (in this case it is equal to 1 bar), η is efficiency factor (dimensionless), k_0 is the pre-exponential factor of the kinetic constant (s^{-1}), E is the activation energy (J mol^{-1}), R is the univeral gas constant (J $mol^{-1}K^{-1}$), ε is the fractional void volume in the catalyst bed (dimensionless).

The values of kinetic parameters (k_0 and E) determined earlier in kinetic experiments over these catalysts (Ismagilov et al, 2008) (see Table 5) were used in the calculations.
The efficiency factor η, accounting for the internal mass transfer limitations, was determined using the standard Thiele equation for the first-order reaction (Malinovskaya et al. 1975).
A heat and mass steady-state model of an ideal displacement adiabatic reactor was used in the simulations of the catalyst bed:

$$u\frac{\partial C_{CH_4}}{\partial \ell} = -W = \beta(C^*_{CH_4} - C_{CH_4}) \tag{3}$$

$$u\frac{\partial T_G}{\partial \ell} = xC^{in}_{CH_4}\Delta T_{AD} = \frac{\alpha}{c_p}(T_C - T_G) \tag{4}$$

$$\ell = 0 \Rightarrow C_i = C_i^{in}; T = T_{in} \tag{5}$$

Here u is the superficial linear gas flow velocity in the reactor reduced to standard conditions and full reactor cross-section area (m/s), ℓ is the coordinate along the reactor height (m), x is the methane conversion, C* and C are methane concentrations at the surface of the catalyst grain and in the gas flow, respectively, β is the mass exchange coefficient for methane (s^{-1}), T_G and T_C are gas and catalyst temperatures (K), correspondingly, ΔT_{AD} is the adiabatic heating of the reaction (K), α is the heat exchange coefficient ($Wm^{-3}\ K^{-1}$), c_p is the gas thermal capacity ($Jm^{-3}\ K^{-1}$), index *in* corresponds to the conditions at the reactor inlet.
The mass and heat transfer coefficients were calculated according to the equations presented in (Aerov et al. 1979) with representation of different catalyst pellets shapes by the spheres of equivalent diameter. Equations used for calculations are presented in detail elsewhere (Ismagilov et al., 2008; Ismagilov et al., 2010).

6.2 Selection of shape and size of catalyst granules

The ultra-low emission characteristics of catalytic combustion chamber are determined not only by the catalyst activity but also by geometric parameters of the catalyst package, such as the bed height and the shape and size of catalyst granules, which are responsible for the efficiency of mass and heat transfer in the fixed catalyst bed. Therefore, the effects of the catalyst granule shape and size on characteristics of the process of catalytic methane combustion: methane conversion, temperature in the bed and pressure drop were studied. Modeling of the process was performed taking into account the influence of the internal and external diffusion on the kinetic parameters (k_0 and E) for the reaction $CH_4 + 2O_2 \rightarrow CO_2 + 2H_2O$ proceeding on each individual catalyst. The calculations were performed for typical operation conditions of the CCC (Parmon et al., 2007): methane concentration in methane–air mixture 1.5 vol.%, GHSV = 5000–40,000 h^{-1} and inlet temperature 723–873 K. The model CCC was represented by a tubular reactor with 80 mm inner diameter and 300 mm catalyst bed height.
The methane combustion modeling shows that the shape of the catalyst granules has a substantial effect on methane conversion, and hence on the residual methane content and the temperature in the catalyst bed. This effect increases with a decrease of the inlet temperature and an increase of the space velocity, being most marked for catalysts with

lower activity. Fig. 9 shows simulated profiles of the residual methane content upon methane oxidation in uniform beds of the IK-12-61 catalysts with different shape: ring

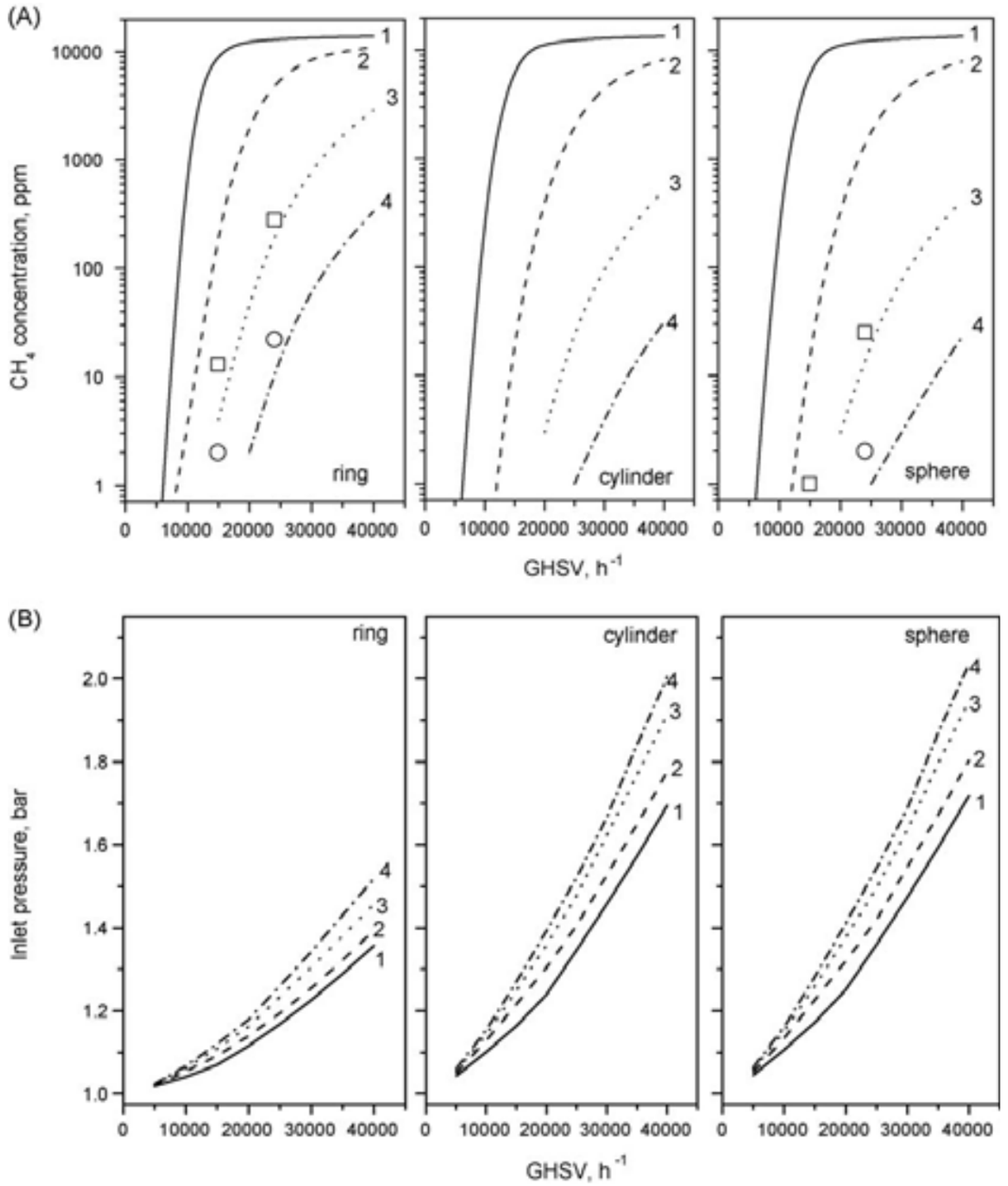

Fig. 9. Simulated profiles of residual methane concentration (A) and inlet pressures (B) vs. GHSV at temperatures: 723 K (Curve 1), 773 K (Curve 2), 823 K (Curve 3) and 873 K (Curve 4) for uniform catalyst package loaded with Mn-La-Al_2O_3 catalyst (IK-12-61) as ring, spherical, and cylindrical granules with size 7.5 mm x 7.5 mm x 2.5 mm, 5.0 mm, and 4.5 mm x 5 mm, respectively. The CCC diameter is 80 mm and the height is 300 mm. Methane concentration is 1.5 vol.%, α = 6.9. Experimental data are presented for comparison: 773 K (□) and 873 K (O).

(7.5 mm × 7.5 mm × 2.5 mm), cylinder (4.5 mm × 5.0 mm) and sphere (5.0 mm). At 723 K and 10,000 h^{-1}, the residual methane contents attained in the beds of spherical and ring-shaped granules of IK-12-61 catalyst are different by a factor of 4.5, but neither of the catalyst shapes provides the required methane emission level (not exceeding 10 ppm) at GHSV higher than 5000 h^{-1}. At higher GHSV, the required methane residual concentration is attained only at the increase of the inlet temperature with a similar effect of the granule shape. For instance, at GHSV below 20,000 h^{-1} the residual methane content less than 10 ppm is observed at the inlet temperature of 823 K for the beds of both ring-shaped and spherical granules, while at 35,000 h^{-1} this methane concentration is attained only on the spherical granules and at a higher temperature of 873 K.

According to modeling, the methane conversion increases with the change of granule shape in the sequence: ring < cylinder < sphere. However, the use of cylindrical and spherical catalyst for the entire reactor is impossible due to a high pressure drop (Fig. 9B). As shown in Fig. 9B, catalytic packages with a height of 300 mm containing ring-shaped and spherical granules give the pressure loss of up to 0.5 and 1.2 bar, respectively.

Thus, in the loading of the CCC with granulated catalysts, the attention should be paid not only to the ultra-low emission characteristics, but also to the minimization of the pressure drop in the catalyst bed. The structured combined catalytic package containing two or three catalysts with optimal catalytic properties and geometrical parameters seems to be promising to meet these two requirements. In design of a combined catalytic package with a high efficiency and a long lifetime, first of all, the light-off temperature and the operation temperature limit of the catalysts should be taken into account, because the CCC having a low light-off temperature of lean methane–air mixtures and high thermal stability provides stable combustion of methane–air mixtures and low emission characteristics. It should be noted that at high inlet temperatures and high methane concentrations the maximum temperature in the catalyst bed can be as high as 1373–1473 K, which can result in the reduction of the catalyst lifetime. Further, three types of catalyst packages complying with the above requirements are examined.

6.3 Variation of the structure of combined catalyst loading in the CCC

6.3.1 Two high temperature catalysts with different granule shapes

The reactor consists of two sections: the first one with the ring shaped oxide catalyst Mn-La-Al_2O_3 or this catalyst modified by Pd (0.5–0.8 wt.%), and the second downstream section with the spherical catalyst having lower fractional void volume. This combination with a shorter bed of spherical catalyst (about 20%) provides rather high methane combustion efficiency at a minor increase of pressure drop (not exceeding 20%) in comparison with the uniform catalytic package. For example, at 40,000 h^{-1} and 873 K, the residual CH_4 content decreased twice and the pressure drop increased only by 18%, when 20% of the ring-shaped Mn-La-Al_2O_3 catalyst was replaced by the spherical granules (Figs. 9A and 10A).

The simulation of methane combustion process shows that the catalytic package with Pd-Mn-La-Al_2O_3 (Fig. 10B) is more effective than the one with Mn-La-Al_2O_3 (Fig. 10A). At similar conditions, the former provides the residual methane concentration 10 times lower than the latter, methane content being below 10 ppm at 25,000 h^{-1} and a temperature as low as 773 K. This catalytic package has also high efficiency at 40,000 h^{-1}, although at a higher inlet temperature (873 K). The catalytic packages with both Pd-Mn-La-Al_2O_3 and Mn-La-Al_2O_3 have a similar thermal stability at temperatures up to 1373 K.

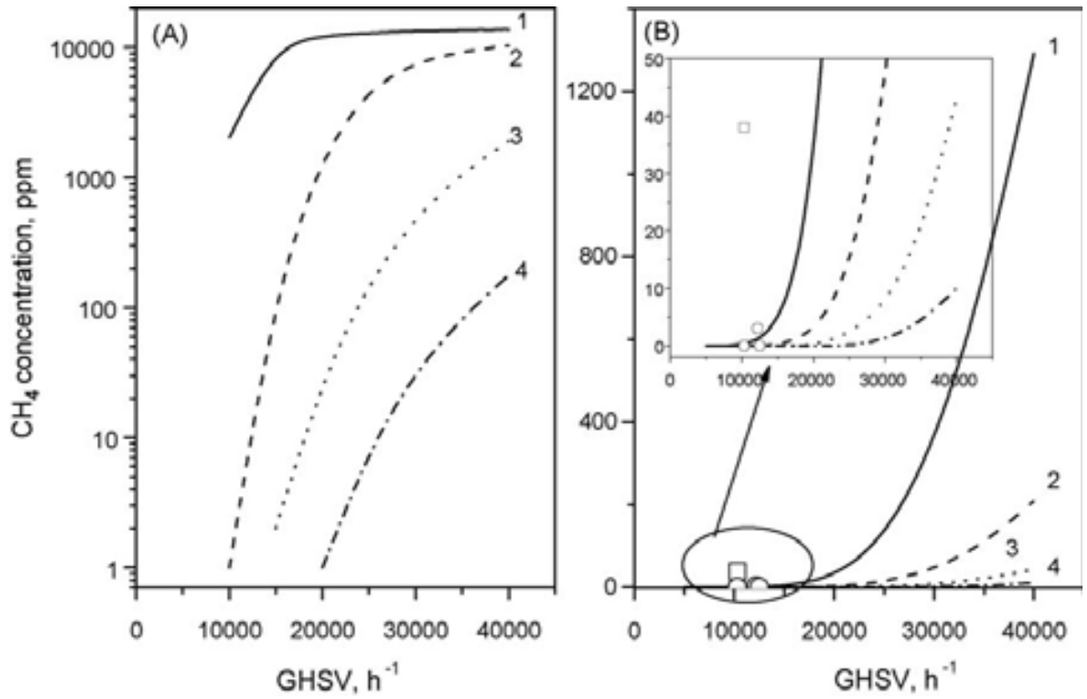

Fig. 10. Simulated profiles of residual methane concentration vs. GHSV at temperatures: 723 K (Curve 1), 773 K (Curve 2), 823 K (Curve 3) and 873 K (Curve 4) for combined catalyst package loaded with Mn-La-Al_2O_3 (A) and Pd-Mn-La-Al_2O_3 (B) catalysts in accordance with Scheme 2 {ring (7.5 mm x 7.5 mm x 2.5 mm), L = 280 mm} + {sphere (5.0 mm), L = 60 mm}. Methane concentration is 1.5 vol.%, α = 6.9. Experimental data are presented for comparison: 743 K (□) and 853 K (O).

6.3.2 Two ring shaped catalysts with different catalytic activity

In this case, a short ignition bed (ca. 10%) of the highly active Pd catalyst is located in the upstream section with a lower temperature. The larger bed of high temperature tolerant Mn-La-Al_2O_3 or Pd-Mn-La-Al_2O_3 catalyst in the downstream section provides practically total methane combustion. This design of the catalyst package allows a reduction of the total Pd loading and an increase of methane combustion efficiency at low inlet temperatures.

Modeling of methane combustion process shows that the use of Pd-CeO_2-Al_2O_3 catalyst is more preferable; however the catalyst package formed from Pd-Mn-La-Al_2O_3 is also rather efficient. The location of a more active catalyst in the upstream section is more advantageous in comparison with a variant of its downstream location (Fig. 11). For example, at the same conditions of 40,000 h^{-1} and 873 K, the simulated residual methane content achieved over the former package does not exceed 10 ppm, while with the latter it is as high as 125 ppm. The effect of the variation of the length of the two sections and space velocity on the process parameters was also studied and showed that the optimal loading of highly active Pd catalyst is close to 10% of the total catalyst loading of the CCC.

6.3.3 Three catalysts with different catalytic activity and fractional void volume

The highly active Pd catalyst in the upstream section initiates methane oxidation, the high temperature tolerant catalyst in the larger middle section provides stable methane

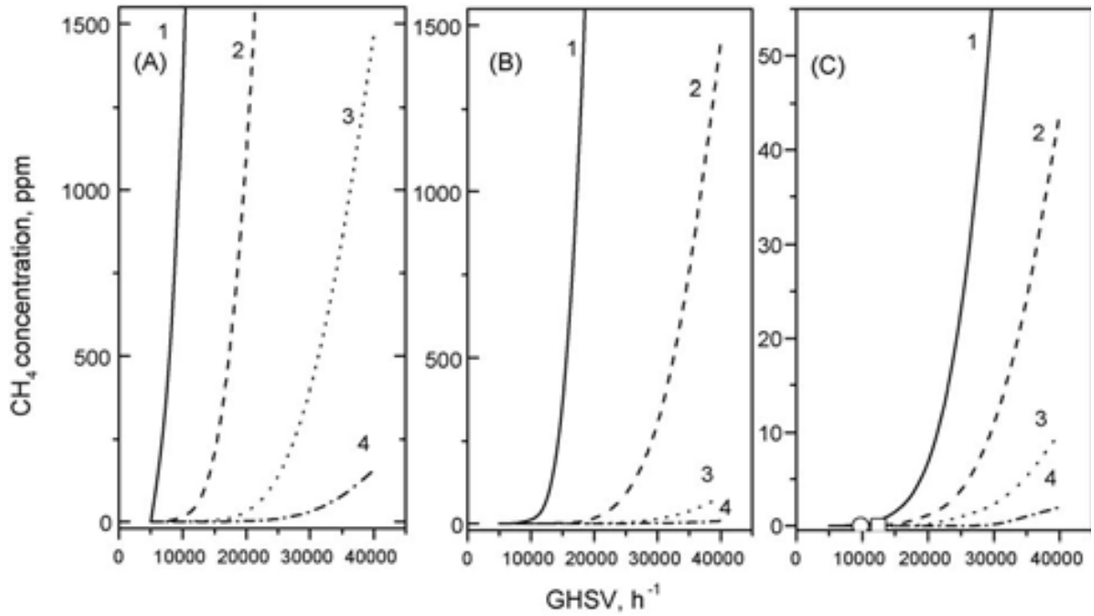

Fig. 11. Simulated profiles of residual methane concentration vs. GHSV at temperatures: 723 K (Curve 1), 773 K (Curve 2), 823 K (Curve 3) and 873 K (Curve 4) for combined catalyst packages in accordance with Scheme 3 (A and B) and Scheme 4 (C). Methane concentration is 1.5 vol.%, α = 6.9. Experimental data are presented for comparison: 743 K (□) and 853 K (O). (A) Mn-La-Al_2O_3 {ring 7.5 mm x 7.5 mm x 2.5 mm, L = 260 mm} + Pd-Mn-La-Al_2O_3 {ring 7.5 mm x 7.5 mm x 2.5 mm, L = 40 mm}, (B) Pd-Mn-La-Al_2O_3 {ring 7.5 mm x 7.5 mm x 2.5 mm, L = 260 mm} + Mn-La-Al_2O_3 {ring 7.5 mm x 7.5 mm x 2.5 mm, L = 40 mm}, (C) Pd-CeO_2-Al_2O_3 {ring 7.5 mm x 7.5 mm x 2.5 mm, L = 40 mm} + Mn-La-Al_2O_3 {ring 7.5 mm x 7.5 mm x 2.5 mm, L = 240 mm} + Pd-Mn-La-Al_2O_3 {sphere 5.0 mm, L = 60 mm}.

combustion. The bicomponent Pd-Mn-La-Al_2O_3 catalyst with a low Pd content and low fractional void volume in the downstream section improves the efficiency by removal of methane residual traces.

The modeling showed that the substitution of 10% of Mn-La-Al_2O_3 catalyst (Fig. 10A) for Pd-CeO_2-Al_2O_3 in the upstream section and the introduction of spherical Pd-Mn-La-Al_2O_3 catalyst in the downstream section of the catalytic package (Fig. 11C) allow a decrease of the inlet temperature and an increase of GHSV. For example, at 20,000 h^{-1} the inlet temperature can be reduced from 873 to 723 K. For the package operation at a higher GHSV (30,000 h^{-1}), an increase of the inlet temperature to 773 K is required. It should be noted that the cost of the combined catalyst package is not significantly higher than that of the uniform Mn-La-Al_2O_3 catalyst bed.

6.4 Comparison of simulated and experimental data

Experimental runs with a model reactor (1.3 l catalyst) demonstrated very good correlation with the results of the modeling (Figs. 9A, 10B and 11C). The catalytic package with the spherical or ring-shaped granules of the IC-12-61 catalyst provided methane combustion to 1 ppm and 15 ppm residual methane concentration, respectively, in the pilot test installation at 15,000 h^{-1} and 773 K and to 2 ppm at 24,000 h^{-1} and 873 K (Fig. 9).

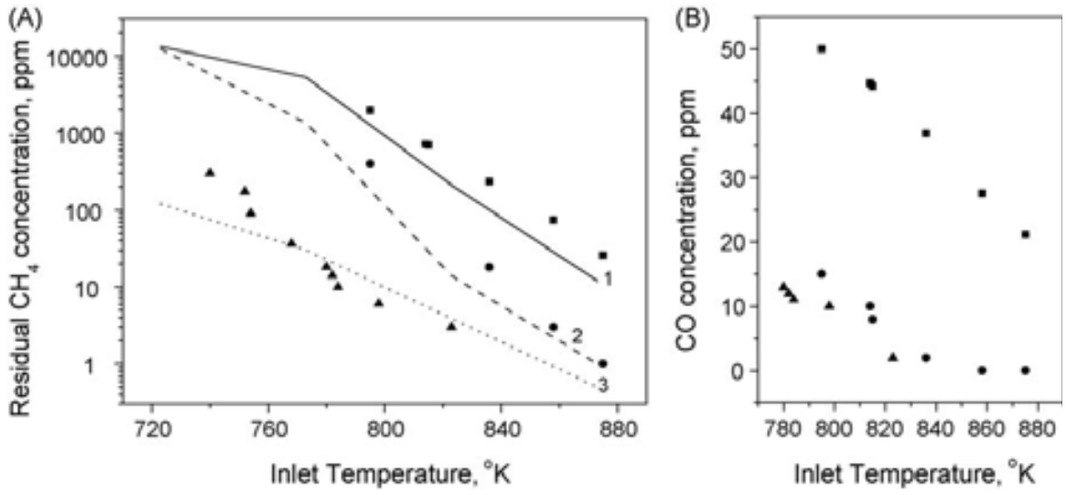

Fig. 12. Residual methane concentration (A) and CO concentration (B) vs. inlet temperature of CCC at GHSV = 24,000 h^{-1} and α = 6.8. Uniform catalyst package loaded with Mn-La-Al_2O_3 catalyst (IK-12-61) as rings (■, Curve 1) and spheres (●, Curve 2), having size 7.5 mm x 7.5 mm x 2.5 mm and 5 mm, respectively, and Pd-Mn-La-Al_2O_3 catalyst (IK-12-62-2) as rings (▲, Curve 3) with size 7.5 mm x 7.5 mm x 2.5 mm. The symbols are experimental data, the lines are calculated data.

Figure 12 shows the correlation between the simulated and experimental data for the residual methane concentrations in a uniform catalytic package with the ring-shaped Mn-La-Al_2O_3 and Pd-Mn-La-Al_2O_3 catalysts at 24,000 h^{-1} as a function of the inlet temperature. The observed deviation of the experimental data on residual methane content from the simulated curves can be explained by two causes. The excess of the experimental values over the simulated ones can be caused by the heat loss. Lower experimental values of the residual methane content in comparison with the calculated ones for the catalyst Pd-Mn-La-Al_2O_3 in the range of the inlet temperatures 773–823 K are probably due to the contribution of other heterogeneous reactions (different from deep oxidation) and gas-phase homogeneous methane oxidation. The carbon dioxide reforming and the partial methane oxidation as well as gas phase reactions have not been incorporated into our simulation yet, because we have not observed CO and H_2 formation in the kinetic experiments (Ismagilov et al., 2008). Noticeable amount of CO (10–14 ppm, Fig. 12B) was observed in the pilot test installation when the CCC was loaded by ring-shaped and/or spherical catalyst granules with a size 7.5 mm x 7.5 mm x 2.5 mm and 5 mm, respectively.

Carbon monoxide can be formed as an intermediate product of homogeneous methane oxidation, which has been shown in the study of methane oxidation in lean mixtures at 900–1400 K (Reinke et al., 2005). Our assumption about the contribution of gas phase methane oxidation agrees with a decrease of the CO concentration when the ring-shaped granules are totally (Fig. 12B) or partially substituted (Fig. 13B) for spherical granules. The ring-shaped and spherical granules are different by the specific external surface (593 and 693 m^{-1}, respectively) and the void fraction in the catalyst bed (ε = 0.5 and 0.42, respectively). It is well known that the increase of the surface and the reduction of the void fraction lead to an increase of free radical decay.

On the other hand, there is strong evidence that the catalyst surface affects the gas-phase chemistry (Sidwell et al., 2003; Deutschmann et al., 2000; Chou et al., 2000; Aghalayam et al.,

2003; Quiceno et al., 2000). The hexaaluminate catalyst surface is assumed to act as a sink for methyl radicals, suppressing gas-phase reactions (Sidwell et al., 2003). The authors made this assumption from comparison of the experimental data with numerical models that include both surface and gas phase chemistry. We also observed that the CO concentration changes along the catalyst bed increasing with the temperature increase up to 1173 K but decreasing at the further rise of the temperature (Fig. 13). The arched profile of the formed CO can be evidence that CO is the intermediate in the multi-step surface reactions mechanism proposed by Deutschmann and coworkers (Deutschmann et al., 2000; Quiceno et al., 2000), Chou et al. (Chou et al., 2000) and Aghalayam (Aghalayam et al., 2003) for the oxidation of lean methane–air mixtures.

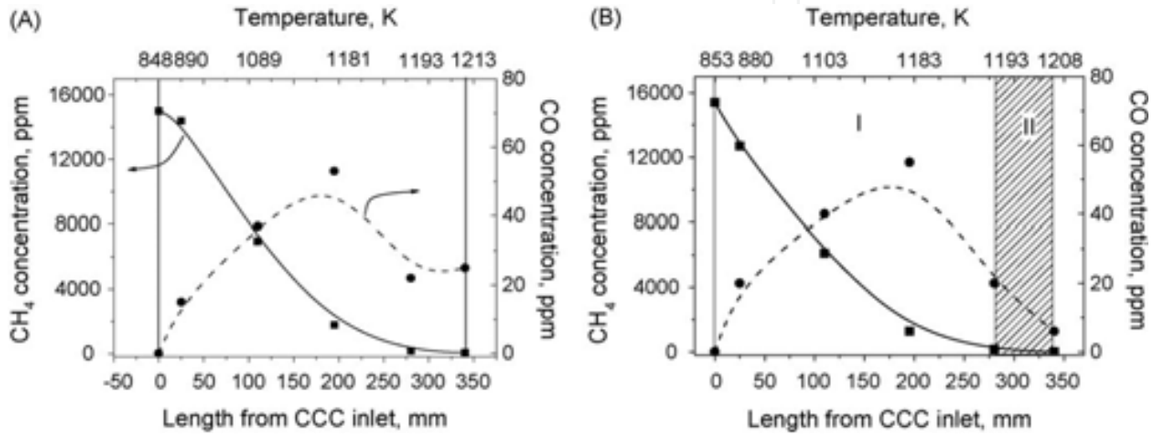

Fig. 13. Profiles of methane (■) and CO (●) concentrations and temperatures along the CCC length during combustion of natural gas in a combined catalyst package: (A) Scheme 1: Pd-Mn-La-Al_2O_3 (ring, 340 mm) at T_{in} = 575°C, GHSV = 15,000 h^{-1}, α = 6.8; (B) Scheme 2: Pd-Mn-La-Al_2O_3 (ring, 280 mm)/Pd-Mn-La-Al_2O_3 (sphere, 60 mm) at Tin = 580°C, GHSV = 15,000 h^{-1}, α = 6.9.

7. Development and testing of a prototype catalytic combustor

Based on the research results a prototype catalytic combustor for a gas turbine with a power 400 kW was designed and fabricated at CIAM (Perets et al., 2009) (Fig. 14). The combustor has a preheating chamber to heat the catalyst to ignition temperature by hot combustion gases and an annular catalyst module with a catalyst loading of 70 kg.

Testing of the prototype combustor demonstrated high efficiency of methane combustion (>99.97%) and low emission of toxic compounds: NOx 0-5 ppm, CO 4-6 ppm, HC 6-20 ppm at inlet temperature 835-880 K, outlet temperature 1145-1160 K, GHSV = 27000-31200 h^{-1}, α = 6.78-7.13, pressure 5 atm (Table 7). It should be noted that nitrogen oxides appeared at all and at low concentrations only if a part of fuel was burned in the preheater.

8. Conclusion

Granular catalysts for natural gas combustion in gas turbine power plants were developed: Pd-Ce-Al_2O_3 catalyst for initiation of methane combustion at low temperatures and the catalysts based on oxides of Mn, hexaaluminates of Mn and La for high temperature

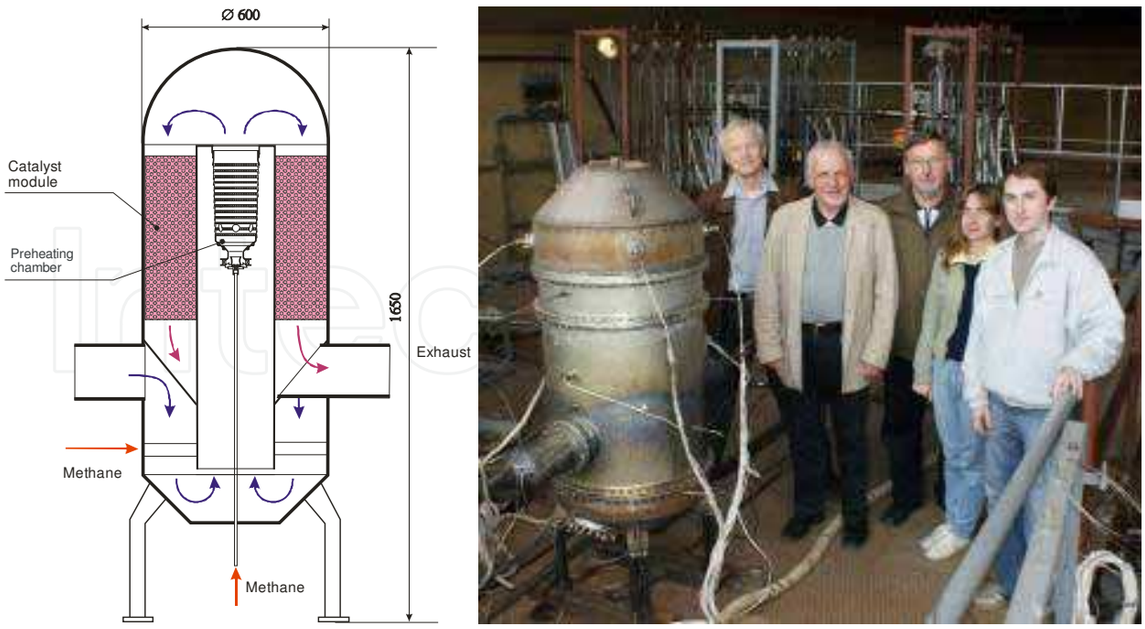

Fig. 14. Scheme and photo of the prototype gas turbine catalytic combustor

Characteristic		Regime 1 Initial test	Regime 2 Modified combustor
Temperature at the combustor inlet		880 K	840 K
Pressure at the combustor inlet		5.0 atm	5.0 atm
Air flow velocity at the combustor inlet		830 g/s (2310 nm^3/h)	960 g/s (2670 nm^3/h)
Methane flow velocity in the preheating chamber		0 g/s (0 nm^3/h)	0.89 g/s (4.5 nm^3/h)
Methane flow velocity in the combustor		6.9 g/s (37.5 nm^3/h)	7.45 g/s (37.5 nm^3/h)
GHSV		27000 h^{-1}	31200 h^{-1}
Air/fuel equivalence ratio		7.13	6.78
Temperature at the catalyst bed inlet		835-860 K	880 K
Temperature at the catalyst bed outlet		1145-1160 K	1145 K
Concentrations at the combustor outlet	HC	18-20 ppm	6 ppm
	CO	4.2-6.0 ppm	4.2 ppm
	NO_x	0 ppm	4.6 ppm

Table 7. Results of tests of the prototype catalytic combustor

methane combustion. The catalytic combustion of natural gas over uniform and combined loadings of granulated manganese-oxide and palladium-containing catalysts was studied for optimization of the design of a catalytic package for use in CCC. The catalysts based on manganese–hexaaluminate showed high efficiency and thermal stability during combustion of natural gas for more than 200 h at the temperature in the catalyst bed as high as 1223-1258 K.

Different schemes of catalytic packages were designed. Modeling of methane combustion in several types of catalyst packages composed of 1, 2 or 3 beds of granulated catalysts with different chemical compositions, shapes and sizes of pellets has been performed.
Granules in the form of rings with dimensions 7.5mm×7.5mm×2.5mm were shown to be the optimal form of the catalysts. At the catalyst package height 300 mm and GHSV= 8,500–15,000 h^{-1} the pressure drop in the catalyst package was lower than 40 mbar. This is less than 4% of the total pressure in CCC (1 bar). The use of 4-5 mm spherical granules in the combined loading increased the pressure drop to 48 mbar at GHSV= 12,500 h^{-1} and 30 mbar at GHSV= 10,000 h^{-1}. However, the use of a thin layer of such granules (less than 17.5%) is acceptable for afterburning residual unburned fuel and CO at the CCC exit.
The highly active Pd-Ce-Al_2O_3 and Pd-Mn-La-Al_2O_3 catalysts should be used in the CCC upstream section for the initiation of methane oxidation. The Mn-La-Al_2O_3 and Pd-Mn-La-Al_2O_3 catalysts with hexaaluminate structure exhibiting good high-temperature activity and high thermal stability can be recommended for the stable methane combustion at a high combustion efficiency in the CCC downstream section. The replacement of 20% of the ring-shaped Mn-La-Al_2O_3 catalyst by the spherical low-percentage Pd-hexaaluminate catalyst in the exit part of the CCC downstream section results in improvement of methane combustion efficiency at a minor increase of the pressure drop (not exceeding 20%). The addition of 10% of the highly active Pd-CeO_2-Al_2O_3 and Pd-Mn-La-Al_2O_3 catalysts with ring shape in the CCC upstream section of such catalytic package provides the required emission characteristics (CH < 10 ppm) at the low inlet temperature (about 723 K) and the high GHSV of lean methane–air mixtures (>20,000 h^{-1}). Experimental runs in the pilot reactor (1.3 kg catalyst) demonstrated very good correlation with the results of the modeling.
Based on the research results a prototype catalytic combustor for a gas turbine with a power 400 kW was designed and fabricated. Experimental runs with a prototype combustor demonstrated high efficiency of methane combustion (>99.97%) and low emission of toxic compounds: NOx < 1 ppm, CO < 10 ppm, HC < 10 ppm.

9. Acknowledgments

This study was supported by Integration projects of RAS Presidium 7.4 and 19.4, RFBR (Grants 06-08-00981 and 07-08-12272) and State Contract 02.526.12.6003

10. References

Aerov, M.E.; Todes, O.M. & Narinskii, M.A. (1979). *Apparaty so statsionarnym zernistym sloem: Gidravlicheskie i teplovye osnovy raboty (Fixed-Bed Apparatuses: Hydraulic and Thermal Principles of Their Operation)*, Khimiya, Moscow

Aghalayam, P.; Park, Y. K.; Fernandes, N.; Papavassiliou, V.; Mhadeshwar, A. B. & Vlachos, D.G. (2003). A C1 mechanism for methane oxidation on platinum. *J. Catal.*, 213, pp. 23-38, 0021-9517

Arai, H.; Yamada, T.; Equchi, K. & Seiyama, T. (1986). Catalytic Combustion of Methane over Various Perovskyte-Type Catalysts. *Appl. Catal.* , A26, pp. 265-279, 0166-9834

Baldwin, T.R. & Burch, R. (1990). Catalytic combustion of methane over supported palladium catalysts *Appl. Catal.*, 1990, vol. 66, 337-358, 0166-9834

Burch, R & Hayes M.J. (1995). C–H bond activation in hydrocarbon oxidation on solid catalysts. *J. Mol. Catal. A*, 100, pp. 13–33, 1381-1169

Burch, R. (1996). Low NOx options in catalytic combustion and emission control. *Pure Appl. Chem*., 68, p. 377-385, 0033-4545

Carroni, R.; Schimdt V. & Griffin T. (2002). Catalytic combustion for power generation. *Catal. Today,* 75, pp. 287-295, 0920-5861

Carroni, R.; Griffin, T.; Mantzaras, J. & Reinke, M. (2003). High-pressure experiments and modeling of methane/air catalytic combustion for power generation applications. *Catal. Today*, 83, pp. 157–170, 0920-5861

Chou, C.P.; Chen, J.Y.; Evans, G.H. & Winters, W.S. (2000). Numerical studies of methane catalytic combustion inside a monolith honeycomb reactor using multi-step surface reactions. *Combust. Sci. Technol*, 150, pp. 27-57, 0010-2202

Chouldhary, T.V.; Banerjee, S. & Choudhary, V.R. (2002). Catalysts for combustion of methane and lower alkanes. *Appl. Catal., A*, 234, pp. 1-23, 0926-860X

Correa, S. (1992). A Review of NO_x Formation Under Gas-Turbine Combustion Conditions. *Combust. Sci. Tech.*, 87, pp. 327-362, 0010-2202

Dalla Betta, R.A.; Schlatter, J.C.; Yee, D.K. ; Loffler, D.G. & Shoji, T. (1995). Catalytic Combustion Technology to Achieve Ultra Low NOx Emissions: Catalyst Design and Performance Characteristics. *Catal. Today*, 26, pp. 329-335, 0920-5861

Dalla Betta, R.A. & Tsurumi K. (1993). Graded palladium-containing partial combustion catalyst and a process for using it. *US patent,* 5,248,251

Dalla Betta, R.A. & Tsurumi, K. (1995) Partial combustion catalyst of palladium on a zirconia support and a process for using it, *US patent* 5,405,260

Dalla Betta R.A. & Rostrup-Nielsen T. (1999). Application of catalytic combustion to a 1.5 MW gas turbine. *Catal. Today.* 47, pp. 369-375, 0920-5861

Dalla Betta, R.A. & Velasco M.A. (2002). Method of thermal NO_x reduction in catalytic combustion systems, *US patent,* 6,718,772

Deutschmann, O.; Maier, L.I.; Riedel, U.; Stroemman A.H. & Dibble, R.W. (2000). Hydrogen assisted catalytic combustion of methane on platinum. *Catal. Today*, 59, 141-150, 0920-5861

Farrauto, R. J., Hobson, M.C., Kennelly, T. and Waterman, E. M. (1992). Catalytic hemistry of Supported Palladium for Combustion of Methane. *Appl. Catal. A*, 81, 227-237, 0926-860X

Groppi, G.; Cristiani, C.; Lietti, L., Ramella, C.; Valentini, M. & Forzatti, P. (1999). Effect of ceria on palladium supported catalysts for high temperature combustion of CH_4 under lean conditions. *Catal. Today*, 50, pp. 399-412, 0920-5861

Hayashi, S.; Yamada, H. & Shimodaira K. (1995). High-pressure reaction and emissions characteristics of catalytic reactors for gas turbine combustors. *Catal. Today*, 26, pp. 319-327, 0920-5861

Ismagilov, Z.R. & Kerzhentsev, M.A. (1990). Catalytic Fuel Combustion - A way of Reducing Emission of Nitrogen Oxides. *Catal. Rev. Sci. Eng.*, 32(1-2), pp. 51-103, 0161-4940

Ismagilov, Z.R.; Shepeleva, M.N.; Shkrabina, R.A. & Fenelonov, V.B. (1991). Interrelation between structural and mechanical characteristics of spherical alumina granules and initial hydroxide properties. *Appl. Catal.* 69, pp. 65 – 73, 0166-9834

Ismagilov, Z.R.; Shkrabina, R.A.; Barannik, G.B. & Kerzhenzev, M.A. (1995). New catalysts and processes for environmental protection. R*eact. Kinet. Catal. Lett.,* 55, 2, pp. 489 – 499, 0133-1736

Ismagilov, Z.R. & Kerzhentsev, M.A. (1999). Fluidized Bed Caytalytic Combustion. *Catal. Today,* 47, pp. 339-346, 0920-5861

Ismagilov, Z.R.; Kerzhentsev, M.A.; Sazonov, V.A.; Tsikoza, L.T.; Shikina, N.V.; Kuznetsov, V.V.; Ushakov, V.A.; Mishanin, S.V.; Kozhukhar, N.G.; Russo, G. & Deutschmann, O. (2003). Study of Catalyts for Catalytic Burners for Fuel Cell Power Plant Reformers. *Korean J. Chem. Eng*., 20, pp. 461-467, 0256-1115

Ismagilov, Z.R; Shikina, N.V.; Yashnik, S.A.; Zagoruiko, A.N.; Khairulin, S.R.; Kerzhentsev, M.A.; Korotkikh, V.N.; Parmon, V.N.; Braynin, B.I.; Zakharov, V.M. & Favorski, O.N. (2008). *Kinet. Catal.* 49, 6, pp. 873-885, 0023-1584

Ismagilov, Z.R.; Shikina, N.V.; Yashnik, S.V.; Parmon, V.N.; Braynin, B.I.; Zakharov, V.M.; Khritov, K.M. & Favorski, O.N. (2009). Method of Burning Hydrocarbon Fuels (Versions) and Catalysts to This End. *Patent of RF*, RU2372556

Ismagilov, Z.R.; Shikina, N.V.; Yashnik, S.A.; Zagoruiko, A.N.; Kerzhentsev, M.A.; Ushakov, V.A.; Sazonov, V.A.; Parmon, V.N.; Zakharov, V.M.; Braynin, B.I. & Favorski, O.N. (2010). *Catal. Today,* http://dx.doi.org/10.1016/j.cattod.2010.04.008 online publication, 0920-5861

Koryabkina, N.A.; Ismagilov, Z.R.; Shkrabina, R.A.; Moroz, E.M. & Ushakov, V.A. (1991). Influence of the method of alumina modification on formation of low-temperature solid solution in magnesia-alumina systems. *Appl. Catal.,* 72, pp. 63 – 69, 0166-9834

Koryabrina, N.A.; Shkrabina, R.A.; Ushakov, V.A. & Ismagilov, Z.R. (1996). Synthesis of a mechanically strong and thermally stable alumina support for catalysts used in combustion processes. *Catal. Today*, 29. pp. 427 – 431, 0920-5861

Jang, B.W.-L.; Nelson, R.M.; Spivey, J.J.; Ocal, M.; Oukaci, R. & Marcelin, G. (1999). Catalytic oxidation of methane over hexaaluminates and hexaaluminate-supported Pd catalysts. *Catal. Today,* 47, pp. 103-113, 0920-5861

Lee, J. H. & Trimm, D. L. (1995). Catalytic Combustion of Methane. *Fuel Process. Technol.,* 42, pp. 339–359, 0378-3820

Liotta, L. F. & Deganello, G. (2003) Thermal stability, structural properties and catalytic activity of Pd catalyst support on Al_2O_3-CeO_2-BaO mixed oxides prepared by sol-gel method. *J. Molec. Catal. A,* 204-205 , pp. 763-770, 1381-1169

Lyubovsky, M. & Pfefferle, L.(1998). Methane combustion over the -alumina supported Pd catalyst: Activity of the mixed Pd/PdO state. *Appl. Catal.,*173, pp. 107-119, 0166-9834

Lyubovsky, M. & Pfefferle, L. (1999). Complete methane oxidation over Pd catalyst supported on alpha.-alumina. Influence of temperature and oxygen pressure on the catalyst activity. *Catal. Today,* 47, pp. 29-44, 0920-5861

Machida, M.; Eguchi, K. & Arai, H. (1987). Effect of additives on the surface area of oxides supports for catalytic combustion. *J. Catal.*, 103, pp. 385-393, 0021-9517

Machida M, Eguchi K, and Arai H. (1989). Catalytic properties of $BaMnAl_{11}O_{19-\delta}$ (M = Cr, Mn, Fe, Co and Ni) for high-temperature catalytic combustion. *J, Catal.,* 1989, 120, pp. 377-386, 0021-9517

Malinovskaya, O.A.; Beskov, V.S. & Slin'ko, M.G. (1975). *Modelirovanie kataliticheskikh protsessov na poristykh zernakh (Modeling of Catalytic Processes on Porous Pellets),* Nauka, Novosibirsk

McCarty, J. G. (1995). Kinetics of PdO combustion catalysis. *Catal. Today*, 26, 283-293, 0920-5861

McCarty, J.G.; Gusman, M.D.; Lowe, M.; Hildenbrand, D.L. & Lau, K.N. (1999). Stability of supported metal and supported metal oxide combustion catalysts, *Catal. Today*, 47, pp. 5–17, 0920-5861

McCarty, J.G. & Wong, V. (2000). Catalytic combustion process, *US patent* 6,015,285

Ozawa, Y.; Tochihara, Y.; Nagai, M. & Omi, S. (2003). PdO/Al_2O_3 in catalytic combustion of methane: stabilization and deactivation, *Chem. Eng. Sci.*, 58, 671-677, 0009-2509

Parmon, V.N.; Ismagilov, Z.R. & Kerzhentsev, M.A. (1992). Catalysis in Energy Production. *Perspectives in Catalysis, Chemistry for 21st Century, Monograph*, J.T. Thomas, K.I. Zamaraev (Eds.), Blackwell Scientific Publication, Oxford, pp. 337-357

Parmon, V.N.; Ismagilov, Z.R.; Favorski, O.N.; Belokon, A.A. & Zakharov, V.M. (2007) Application of Catalytic Combustion Chambers in Gas Turbine Units of Decentralized Energy Supply. *Herald Russ. Acad. Sci.*, 77, 819-830

Perets, V.N.; Zakharov V.M.; Favorski, O.N. & Braynin, B.I. (2008). Gas Turbine Plant With Regenerative Cycle And Catalyst Combustion Chamber. *Patent of RF*, RU2342601

Pfefferle, L.D. & Pfefferle, W.C. (1987). Catalysis in Combustion. *Catal. Rev. Sci. Eng.*, 29, pp. 219-267, 0161-4940

Pfefferle, W.C. (1997). Catalytic method. *US patent,* 5,601,426

Quiceno, R.R.; Perez Ramirez, J.; Warnatz, J. & Deutschmann, O. (2000). Modeling the high-temperature catalytic partial oxidation of methane over platinum gauze: detailed gas phase and surface chemistries coupled with 3D flow field simulation. *Applied Catalysis A*: *General,* 303, pp. 166–176, 0926-860X

Reinke, M.; Mantzaras,J.; Bombach R.,; Schenker, S. & Inauen A. (2005). Gas phase chemistry in catalytic combustion of methane/air mixtures over platinum at pressures of 1 bar to 16 bar. *Combustion and Flame*, 141, 448-468, 0010-2180

Sidwell, R.W.; Zhu, H.; Kee, R.J. & Wickham D.T. (2003). Catalytic Combustion of Premixed Methane-in-air on a High Temperature Stagnation Surface," Combustion and Flame, 134, pp. 55-66, 0010-2180

Shepeleva, M.N.; Shkrabina, R.A.; Fenelonov, V.B. & Ismagilov, Z.R. (1991). Production of spherical granules of alumina with controlled porous structure. *Appl. Catal.* 78, 175 – 184, 0166-9834

Su, S.C.; Carstens, J.N.; & Bell, A.T. (1998a). A study of the dynamics of Pd oxidation and PdO reduction by H_2 and CH_4 *J. Catal.,* 176, 125-135, 0021-9517

Su, S.C.; Carstens, J.N.; & Bell, A.T. (1998b). Factors affecting the catalytic activity of Pd/ZrO2 for the combustion of methane *J. Catal.,* 176, 136-142, 0021-9517

Trimm, D. L. (1983). Catalytic combustion (Review). *Appl. Catal.*, 7. No 3, pp. 249-282, 0166-9834

Tsikoza, L.T.; Yashnik, S.A.; Ismagilov, Z.R.; Shkrabina, R.A.; Korjabkina, N.A. & Kuznetsov, V.V. (2002). Catalyst For High-Temperature Combustion Of Hydrocarbon Fuel (Versions). *Patent,* RU 2185238

Tsikoza, L.T.; Ismagilov, Z.R.; Ushakov, V.A.; Kuznetsov, V.V. & Ovsyannikova, I.A. (2003). Fuel Combustion Reactions and Catalysts: XXI. Synthesis and Characterization of Modified Mn–Al–O Catalysts for High-Temperature Oxidation. *Kinet. Catal. (Engl. Transl.),* 44, pp. 806-812, 0023-1584

Yashnik, S.A.; Ismagilov, Z.R.; Kuznetsov, V.V.; Ushakov, V.V.; Rogov, V.A. & Ovsyannikova, I.A. (2006). *Catal. Today*, 117, pp. 525-535, 0920-5861

Yashnik, S.A.; Shikina, N.V.; Ismagilov, Z.R.; Zagoruiko, A.N.; Kerzhentsev, M.A.; Parmon, V.N.; Zakharov, V.M.; Braynin, B.I.; Favorski, O.N. & Gumerov, A.M. (2009). *Catal. Today,* 147S, pp. S237–S243, 0920-5861

Young, W.E. & Carl, D.E. (1989). Passively cooled catalytic combustor for a stationary combustion turbine. *US patent,* 4,870,824

Yue, B.; Zhou, R.; Wang, Y. & Zheng, X. (2005). Effect of rare earths (La, Pr, Nd, Sm and Y) on the methane combustion over Pd/Ce–Zr/Al_2O_3 catalysts. *Appl. Catal., A*, 295, pp. 31-39

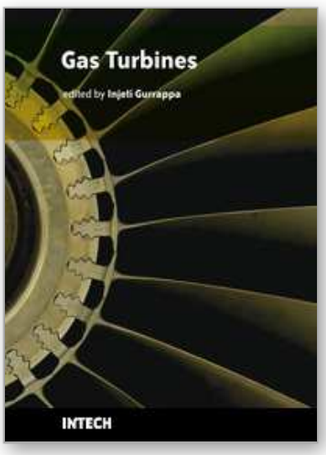

Gas Turbines

Edited by Gurrappa Injeti

ISBN 978-953-307-146-6
Hard cover, 364 pages
Publisher Sciyo
Published online 27, September, 2010
Published in print edition September, 2010

This book is intended to provide valuable information for the analysis and design of various gas turbine engines for different applications. The target audience for this book is design, maintenance, materials, aerospace and mechanical engineers. The design and maintenance engineers in the gas turbine and aircraft industry will benefit immensely from the integration and system discussions in the book. The chapters are of high relevance and interest to manufacturers, researchers and academicians as well.

InTech Europe
University Campus STeP Ri
Slavka Krautzeka 83/A
51000 Rijeka, Croatia
Phone: +385 (51) 770 447
Fax: +385 (51) 686 166
www.intechopen.com

InTech China
Unit 405, Office Block, Hotel Equatorial Shanghai
No.65, Yan An Road (West), Shanghai, 200040, China
中国上海市延安西路65号上海国际贵都大饭店办公楼405单元
Phone: +86-21-62489820
Fax: +86-21-62489821

IntechOpen